

1 **Mitochondrial respiratory states and rates:**  
2 **Building blocks of mitochondrial physiology**  
3 **Part 1.** MitoEAGLE preprint 2018-02-23(29)  
4

5 [http://www.mitoeagle.org/index.php/MitoEAGLE\\_preprint\\_2018-02-08](http://www.mitoeagle.org/index.php/MitoEAGLE_preprint_2018-02-08)  
6

7 Preprint version 29 (2018-02-23)

8 **MitoEAGLE Network**

9 Corresponding author: Gnaiger E

10 Contributing co-authors

11 Aasander Frostner E, Acuna-Castroviejo D, Ahn B, Alves MG, Amati F, Aral C,  
12 Arandarčikaitė O, Bailey DM, Bakker BM, Bastos Sant'Anna Silva AC, Battino M, Beard  
13 DA, Ben-Shachar D, Bishop D, Borutaitė V, Breton S, Brown GC, Brown RA, Buettner GR,  
14 Burtscher J, Calabria E, Calbet JA, Cardoso LHD, Carvalho E, Casado Pinna M, Cervinkova  
15 Z, Chang SC, Chaurasia B, Chen Q, Chicco AJ, Chinopoulos C, Clementi E, Coen PM, Collin  
16 A, Crisóstomo L, Das AM, Davis MS, De Palma C, Dias TR, Distefano G, Doerrier C,  
17 Drahotka Z, Duchon MR, Ehinger J, Elmer E, Endlicher R, Fell DA, Ferko M, Ferreira JCB,  
18 Filipovska A, Fisar Z, Fischer M, Fisher JJ, Fornaro M, Galkin A, Garcia-Roves PM, Garcia-  
19 Souza LF, Genova ML, Giovarelli M, Gonzalez-Arment JL, Gonzalo H, Goodpaster BH,  
20 Gorr TA, Gourlay CW, Granata C, Grefte S, Haas CB, Haavik J, Han J, Harrison DK,  
21 Hellgren KT, Hernansanz-Agustin P, Holland O, Hoppel CL, Houstek J, Hunger M, Iglesias-  
22 Gonzalez J, Irving BA, Iyer S, Jackson CB, Jadiya P, Jang DH, Jansen-Dürr P, Jespersen NR,  
23 Jha RK, Kaambre T, Kane DA, Kappler L, Karabatsiakos A, Keijer J, Keppner G,  
24 Klingenspor M, Komlodi T, Kopitar-Jerala N, Krako Jakovljevic N, Kuang J, Kucera O,  
25 Labieniec-Watala M, Lai N, Laner V, Larsen TS, Lee HK, Lemieux H, Lerfall J, Lucchinetti  
26 E, MacMillan-Crow LA, Makrecka-Kuka M, Malik A, Markova M, Meszaros AT, Michalak  
27 S, Moiso N, Molina AJA, Montaigne D, Moore AL, Moreira BP, Mracek T, Muntane J,  
28 Muntean DM, Murray AJ, Nemeč M, Neuzil J, Newsom S, Nozickova K, O'Gorman D,  
29 Oliveira MT, Oliveira PF, Oliveira PJ, Orynbayeva Z, Pak YK, Palmeira CM, Patel HH,  
30 Pecina P, Pelena D, Pereira da Silva Grilo da Silva F, Pesta D, Petit PX, Pichaud N, Piel S,  
31 Pirkmajer S, Porter RK, Pranger F, Prochownik EV, Pulinilkunnil T, Puurand M, Radenkovic  
32 F, Radi R, Ramzan R, Reboredo P, Renner-Sattler K, Robinson MM, Rohlena J, Ropelle ER,  
33 Røslund GV, Rossiter HB, Rybacka-Mossakowska J, Saada A, Salvadego D, Sandi C,  
34 Scatena R, Schartner M, Scheibye-Knudsen M, Schilling JM, Schlattner U, Schoenfeld P,  
35 Schwarzer C, Scott GR, Shabalina IG, Sharma P, Sharma V, Shevchuk I, Siewiera K, Silber  
36 AM, Singer D, Smenes BT, Soares FAA, Sobotka O, Sokolova I, Spinazzi M, Stankova P,  
37 Stier A, Stocker R, Sumbalova Z, Suravajhala P, Swerdlow RH, Swiniuch D, Tanaka M,  
38 Tandler B, Tepp K, Tomar D, Towheed A, Tretter L, Trifunovic A, Trivigno C, Tronstad KJ,  
39 Trougakos IP, Tyrrell DJ, Urban T, Valentine JM, Velika B, Vendelin M, Vercesi AE, Victor  
40 VM, Villena JA, Vogt S, Volani C, Votion DM, Vujacic-Mirski K, Wagner BA, Ward ML,  
41 Watala C, Wei YH, Wieckowski MR, Williams C, Wohlwend M, Wolff J, Wuest RCI, Zaugg  
42 K, Zaugg M, Zischka H, Zorzano A

43 Supporting co-authors:

44 Bernardi P, Boetker HE, Borsheim E, Bouitbir J, Calzia E, Coker RH, Dubouchaud H,  
45 Durham WJ, Dyrstad SE, Engin AB, Gan Z, Garlid KD, Garten A, Haendeler J, Hand SC,  
46 Hepple RT, Hickey AJ, Hoel F, Kainulainen H, Khamoui AV, Koopman WJH, Kowaltowski  
47 AJ, Krajcova A, Lane N, Lenaz G, Liu J, Liu SS, Mazat JP, Menze MA, Methner A,  
48 Nedergaard J, Pallotta ML, Parajuli N, Pettersen IK, Porter C, Salin K, Sazanov LA, Skolik  
49 R, Sonkar VK, Szabo I, Thyfault JP, Vieyra A  
50  
51

**Updates and discussion:**

[http://www.mitoeagle.org/index.php/MitoEAGLE\\_preprint\\_2018-02-08](http://www.mitoeagle.org/index.php/MitoEAGLE_preprint_2018-02-08)

Correspondence: Gnaiger E

*Chair COST Action CA15203 MitoEAGLE* – <http://www.mitoeagle.org>

*Department of Visceral, Transplant and Thoracic Surgery, D. Swarovski Research Laboratory, Medical University of Innsbruck, Innrain 66/4, A-6020 Innsbruck, Austria*

*Email: erich.gnaiger@i-med.ac.at*

*Tel: +43 512 566796, Fax: +43 512 566796 20*

**Contents****Abstract****Executive summary****1. Introduction** – Box 1: In brief: Mitochondria and Bioblasts**2. Oxidative phosphorylation and coupling states in mitochondrial preparations**

Mitochondrial preparations

*2.1. Respiratory control and coupling*

The steady-state

Specification of biochemical dose

Phosphorylation,  $P_{\gg}$ , and  $P_{\gg}/O_2$  ratio

Control and regulation

Respiratory control and response

Respiratory coupling control and ET-pathway control

Coupling

Uncoupling

*2.2. Coupling states and respiratory rates*

Respiratory capacities in coupling control states

LEAK, OXPHOS, ET, ROX

*2.3. Classical terminology for isolated mitochondria*

States 1–5

**3. Normalization: fluxes and flows***3.1. Normalization: system or sample*

Flow per system,  $I$

Extensive quantities

Size-specific quantities – Box 2: Metabolic fluxes and flows: vectorial and scalar

*3.2. Normalization for system-size: flux per chamber volume*

System-specific flux,  $J_{V,O_2}$

*3.3. Normalization: per sample*

Sample concentration,  $C_{mX}$

Mass-specific flux,  $J_{O_2/mX}$

Number concentration,  $C_{NX}$

Flow per object,  $I_{O_2/X}$

*3.4. Normalization for mitochondrial content*

Mitochondrial concentration,  $C_{mtE}$ , and mitochondrial markers

Mitochondria-specific flux,  $J_{O_2/mtE}$

*3.5. Evaluation of mitochondrial markers**3.6. Conversion: units***4. Conclusions** – Box 3: Mitochondrial and cell respiration**5. References**

102 **Abstract** As the knowledge base and importance of mitochondrial physiology to human health  
103 expands, the necessity for harmonizing nomenclature concerning mitochondrial respiratory  
104 states and rates has become increasingly apparent. Clarity of concept and consistency of  
105 nomenclature are key trademarks of a research field. These trademarks facilitate effective  
106 transdisciplinary communication, education, and ultimately further discovery. Peter Mitchell's  
107 chemiosmotic theory establishes the mechanism of energy transformation and coupling in  
108 oxidative phosphorylation. The unifying concept of the protonmotive force provides the  
109 framework for developing a consistent theory and nomenclature for mitochondrial physiology  
110 and bioenergetics. Herein, we follow IUPAC guidelines on general terms of physical chemistry,  
111 extended by considerations on open systems and irreversible thermodynamics. We align the  
112 nomenclature and symbols of classical bioenergetics with a concept-driven constructive  
113 terminology to express the meaning of each quantity clearly and consistently. In this position  
114 statement, in the frame of COST Action MitoEAGLE, we endeavour to provide a balanced  
115 view on mitochondrial respiratory control and a critical discussion on reporting data of  
116 mitochondrial respiration in terms of metabolic flows and fluxes. Uniform standards for  
117 evaluation of respiratory states and rates will ultimately support the development of databases  
118 of mitochondrial respiratory function in species, tissues, and cells.

119

120 *Keywords:* Mitochondrial respiratory control, coupling control, mitochondrial  
121 preparations, protonmotive force, oxidative phosphorylation, OXPHOS, efficiency, electron  
122 transfer, ET; proton leak, LEAK, residual oxygen consumption, ROX, State 2, State 3, State 4,  
123 normalization, flow, flux, O<sub>2</sub>

124

125

126

---

## 127 **Executive summary**

128

129

130 1. In view of broad implications on health care, mitochondrial researchers face an  
131 increasing responsibility to disseminate their fundamental knowledge and novel  
132 discoveries to a wide range of stakeholders and scientists beyond the group of  
133 specialists. This requires implementation of a commonly accepted terminology  
134 within the discipline and standardization in the translational context. Authors,  
135 reviewers, journal editors, and lecturers are challenged to collaborate with the aim  
136 to harmonize the nomenclature in the growing field of mitochondrial physiology  
and bioenergetics.

137

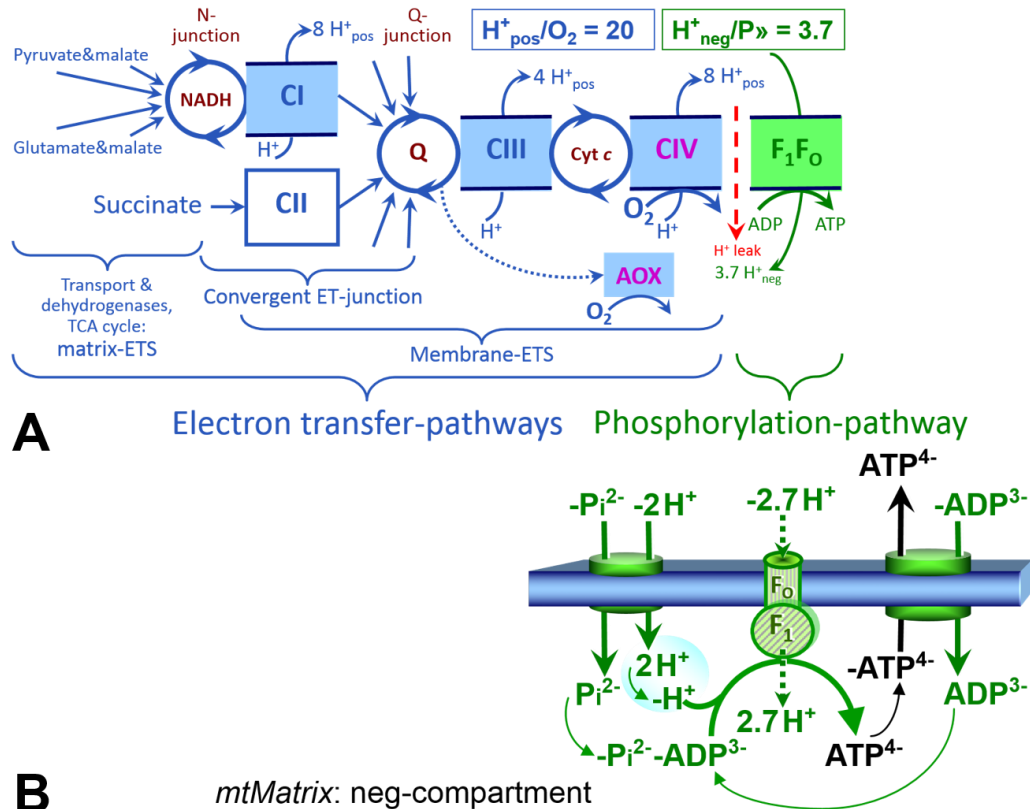
138 2. Aerobic energy metabolism in mammalian mitochondria depends on the coupling of  
139 phosphorylation (ADP → ATP) to O<sub>2</sub> flux in catabolic reactions. In this process of  
140 oxidative phosphorylation, coupling is mediated by translocation of protons  
141 through respiratory proton pumps operating across the inner mitochondrial  
142 membrane and generating or utilizing the protonmotive force measured between  
143 the mitochondrial matrix and intermembrane compartment. Compartmental  
144 coupling thus distinguishes vectorial oxidative phosphorylation from fermentation  
as the counterpart of cellular core energy metabolism.

145

146 3. To exclude fermentation and other cytosolic interactions from exerting an effect on  
147 mitochondrial metabolism, the barrier function of the plasma membrane must be  
148 disrupted. Selective removal or permeabilization of the plasma membrane yields  
149 mitochondrial preparations—including isolated mitochondria, tissue and cellular  
150 preparations—with structural and functional integrity. Then extra-mitochondrial  
151 concentrations of fuel substrates transported into the mitochondrial matrix, ADP,  
ATP, inorganic phosphate, and cations including H<sup>+</sup> can be controlled to determine  
152 mitochondrial function under a set of conditions defined as coupling control states.

153  
154  
155  
156  
157

A concept-driven terminology of bioenergetics incorporates in its terms and symbols explicit information on the nature of respiratory states, that makes the technical terms readily recognized and easy to understand.



158  
159  
160  
161  
162  
163  
164  
165  
166  
167  
168  
169  
170  
171  
172  
173  
174  
175  
176  
177  
178  
179

**Fig. 1. The oxidative phosphorylation (OXPHOS) system.** (A) The mitochondrial electron transfer system (ETS) is fuelled by diffusion and transport of substrates across the mtOM and mtIM and consists of the matrix-ETS and membrane-ETS. ET-pathways are coupled to the phosphorylation-pathway. ET-pathways converge at the N-junction and Q-junction. Additional arrows indicate electron entry into the Q-junction through electron transferring flavoprotein, glycerophosphate dehydrogenase, dihydro-orotate dehydrogenase, choline dehydrogenase, and sulfide-ubiquinone oxidoreductase. The dotted arrow indicates the branched pathway of oxygen consumption by alternative quinol oxidase (AOX). The  $H^+_{pos}/O_2$  ratio is the outward proton flux from the matrix space to the positively (pos) charged compartment, divided by catabolic  $O_2$  flux in the NADH-pathway. The  $H^+_{neg}/P \gg$  ratio is the inward proton flux from the inter-membrane space to the negatively (neg) charged matrix space, divided by the flux of phosphorylation of ADP to ATP (Eq. 1). These are not fixed stoichiometries due to ion leaks and proton slip. (B) Phosphorylation-pathway catalyzed by the proton pump F<sub>1</sub>F<sub>0</sub>-ATPase (F-ATPase, ATP synthase), adenine nucleotide translocase, and inorganic phosphate transporter. The  $H^+_{neg}/P \gg$  stoichiometry is the sum of the coupling stoichiometry in the F-ATPase reaction ( $-2.7 H^+_{pos}$  from the positive intermembrane space,  $2.7 H^+_{neg}$  to the matrix, *i.e.*, the negative compartment) and the proton balance in the translocation of ADP<sup>2-</sup>, ATP<sup>3-</sup> and Pi<sup>2-</sup>. Modified from (A) Lemieux *et al.* (2017) and (B) Gnaiger (2014).

- 180 4. Mitochondrial coupling states are defined according to the control of respiratory oxygen  
 181 flux by the protonmotive force. Capacities of oxidative phosphorylation and  
 182 electron transfer capacities are measured at kinetically saturating concentrations of  
 183 fuel substrates, ADP and inorganic phosphate, or at optimal uncoupler  
 184 concentrations, respectively. Respiratory capacities are a measure of the upper  
 185 bound of the rates of respiration, providing reference values for the diagnosis of  
 186 health and disease, and for evaluation of the effects of **E**volutionary background,  
 187 **A**ge, **G**ender and sex, **L**ifestyle and **E**nvironment (EAGLE).
- 188 5. Some degree of uncoupling is a characteristic of energy-transformations across  
 189 membranes. Uncoupling is caused by a variety of physiological, pathological,  
 190 toxicological, pharmacological and environmental conditions that exert an  
 191 influence not only on the proton leak and cation cycling, but also on proton slip  
 192 within the proton pumps and the structural integrity of the mitochondria. A more  
 193 loosely coupled state is induced by stimulation of mitochondrial superoxide  
 194 formation and the bypass of proton pumps. In addition, uncoupling by application  
 195 of protonophores represents an experimental intervention for the transition from a  
 196 well-coupled to the noncoupled state of mitochondrial respiration.
- 197 6. Respiratory oxygen consumption rates have to be carefully normalized to enable meta-  
 198 analytic studies beyond the specific question of a particular experiment. Therefore,  
 199 all raw data should be published in a supplemental table or open access data  
 200 repository. Normalization of rates for the volume of the experimental chamber (the  
 201 measuring system) is distinguished from normalization for (1) the volume or mass  
 202 of the experimental sample, (2) the number of objects (cells, organisms), and (3)  
 203 the concentration of mitochondrial markers in the chamber.
- 204 7. The consistent use of terms and symbols discussed in this MitoEAGLE position  
 205 statement will facilitate transdisciplinary communication and support further  
 206 development of a database on bioenergetics and mitochondrial physiology. The  
 207 present considerations are focused on studies with mitochondrial preparations.  
 208 These will be extended in a series of reports on pathway control of mitochondrial  
 209 respiration, the protonmotive force, respiratory states in intact cells, and  
 210 harmonization of experimental procedures.

---

### 214 **Box 1: In brief – Mitochondria and Bioblasts**

215 **Mitochondria** are the oxygen-consuming electrochemical generators evolved from  
 216 endosymbiotic bacteria (Margulis 1970; Lane 2005). They were described by Richard Altmann  
 217 (1894) as ‘bioblasts’, which include not only the mitochondria as presently defined, but also  
 218 symbiotic and free-living bacteria. The word ‘mitochondria’ (Greek mitos: thread; chondros:  
 219 granule) was introduced by Carl Benda (1898).

220 We now recognize mitochondria as a dynamic network with a double membrane that are  
 221 contained within eukaryotic cells. The mitochondrial inner membrane (mtIM) shows dynamic  
 222 tubular to disk-shaped cristae that separate the mitochondrial matrix, *i.e.*, the negatively charged  
 223 internal mitochondrial compartment, and the intermembrane space; the latter being positively  
 224 charged and enclosed by the mitochondrial outer membrane (mtOM). The mtIM contains the  
 225 non-bilayer phospholipid cardiolipin, which is not present in any other eukaryotic cellular  
 226 membrane. Cardiolipin promotes the formation of respiratory supercomplexes (SC  $I_nIII_nIV_n$ ),  
 227 which are supramolecular assemblies based upon specific, though dynamic, interactions  
 228 between individual respiratory complexes (Greggio *et al.* 2017; Lenaz *et al.* 2017). Membrane  
 229



230 fluidity exerts an influence on functional properties of proteins incorporated in the membranes  
231 (Waczulikova *et al.* 2007).

232 Mitochondria are the structural and functional elements of cell respiration. Cell  
233 respiration is the reduction of oxygen by electron transfer coupled to electrochemical proton  
234 translocation across the mtIM. In the process of oxidative phosphorylation (OXPHOS), the  
235 catabolic reaction of oxygen consumption is electrochemically coupled to the transformation of  
236 energy in the form of adenosine triphosphate (ATP; Mitchell 1961, 2011). Mitochondria are the  
237 powerhouses of the cell which contain the machinery of the OXPHOS-pathways, including  
238 transmembrane respiratory complexes—proton pumps with FMN, Fe-S and cytochrome *b, c,*  
239 *aa<sub>3</sub>* redox systems); alternative dehydrogenases and oxidases; the coenzyme ubiquinone (Q);  
240 F-ATPase or ATP synthase; the enzymes of the tricarboxylic acid cycle and fatty acid oxidation;  
241 transporters of ions, metabolites and co-factors; and mitochondrial kinases related to energy  
242 transfer pathways. The mitochondrial proteome comprises over 1,200 proteins (Calvo *et al.*  
243 2015; 2017), mostly encoded by nuclear DNA (nDNA), with a variety of functions, many of  
244 which are relatively well known (*e.g.*, apoptosis-regulating proteins), while others are still under  
245 investigation, or need to be identified (*e.g.*, alanine transporter).

246 There is a constant crosstalk between mitochondria and the other cellular components.  
247 The crosstalk between mitochondria and endoplasmic reticulum is involved in the regulation of  
248 calcium homeostasis, cell division, autophagy, differentiation, anti-viral signaling (Murley and  
249 Nunnari 2016). Cellular mitostasis is maintained through regulation at both the transcriptional  
250 and post-translational level, through cell signalling including proteostatic (*e.g.*, the ubiquitin-  
251 proteasome and autophagy-lysosome pathways), and genome stability modules throughout the  
252 cell cycle or even cell death, contributing to homeostatic regulation in response to varying  
253 energy demands and stress (Quiros *et al.* 2016). In addition to mitochondrial movement along  
254 microtubules, mitochondrial morphology can change in response to energy requirements of the  
255 cell via processes known as fusion and fission, through which mitochondria communicate  
256 within a network, and in response to intracellular stress factors causing swelling and ultimately  
257 permeability transition.

258 Mitochondria typically maintain several copies of their own genome known as  
259 mitochondrial DNA (mtDNA; hundred to thousands per cell; Cummins 1998), which is  
260 maternally inherited. Biparental mitochondrial inheritance is documented in mammals, birds,  
261 fish, reptiles and invertebrate groups, and is even the norm in bivalves (Breton *et al.* 2007;  
262 White *et al.* 2008). mtDNA is compact (16.5 kB in humans) and encodes 13 protein subunits  
263 of the transmembrane respiratory Complexes CI, CIII, CIV and F-ATPase, 22 tRNAs, and two  
264 RNAs. Additional gene content has been suggested to include microRNAs, piRNA,  
265 smithRNAs, repeat associated RNA, and even additional proteins (Duarte *et al.* 2014; Lee *et al.*  
266 2015; Cobb *et al.* 2016). The mitochondrial genome requires nuclear-encoded mitochondrial  
267 targeted proteins for its maintenance and expression (Rackham *et al.* 2012).

268 Abbreviation: mt, as generally used in mtDNA. Mitochondrion is singular and  
269 mitochondria is plural.

270 *‘For the physiologist, mitochondria afforded the first opportunity for an experimental*  
271 *approach to structure-function relationships, in particular those involved in active transport,*  
272 *vectorial metabolism, and metabolic control mechanisms on a subcellular level’* (Ernster and  
273 Schatz 1981).

---

275

276

277

## 1. Introduction

278

279 Mitochondria are the powerhouses of the cell with numerous physiological, molecular,  
280 and genetic functions (**Box 1**). Every study of mitochondrial health and disease is faced with

281 **Evolution, Age, Gender and sex, Lifestyle, and Environment (EAGLE)** as essential background  
282 conditions intrinsic to the individual patient or subject, cohort, species, tissue and to some extent  
283 even cell line. As a large and coordinated group of laboratories and researchers, the mission of  
284 the global MitoEAGLE Network is to generate the necessary scale, type, and quality of  
285 consistent data sets and conditions to address this intrinsic complexity. Harmonization of  
286 experimental protocols and implementation of a quality control and data management system  
287 are required to interrelate results gathered across a spectrum of studies and to generate a  
288 rigorously monitored database focused on mitochondrial respiratory function. In this way,  
289 researchers within the same and across different disciplines will be positioned to compare  
290 findings across traditions and generations to an agreed upon set of clearly defined and accepted  
291 international standards.

292 Reliability and comparability of quantitative results depend on the accuracy of  
293 measurements under strictly-defined conditions. A conceptual framework is required to warrant  
294 meaningful interpretation and comparability of experimental outcomes carried out by research  
295 groups at different institutes. With an emphasis on quality of research, collected data can be  
296 useful far beyond the specific question of a particular experiment. Enabling meta-analytic  
297 studies is the most economic way of providing robust answers to biological questions (Cooper  
298 *et al.* 2009). Vague or ambiguous jargon can lead to confusion and may relegate valuable  
299 signals to wasteful noise. For this reason, measured values must be expressed in standard units  
300 for each parameter used to define mitochondrial respiratory function. Harmonization of  
301 nomenclature and definition of technical terms are essential to improve the awareness of the  
302 intricate meaning of current and past scientific vocabulary, for documentation and integration  
303 into databases in general, and quantitative modelling in particular (Beard 2005). The focus on  
304 coupling states and fluxes through metabolic pathways of aerobic energy transformation in  
305 mitochondrial preparations is a first step in the attempt to generate a conceptually-oriented  
306 nomenclature in bioenergetics and mitochondrial physiology. Coupling states of intact cells,  
307 the protonmotive force, and respiratory control by fuel substrates and specific inhibitors of  
308 respiratory enzymes will be reviewed in subsequent communications.

309  
310

## 311 **2. Oxidative phosphorylation and coupling states in mitochondrial preparations**

312 *‘Every professional group develops its own technical jargon for talking about matters of*  
313 *critical concern ... People who know a word can share that idea with other members of*  
314 *their group, and a shared vocabulary is part of the glue that holds people together and*  
315 *allows them to create a shared culture’* (Miller 1991).

316

317 **Mitochondrial preparations** are defined as either isolated mitochondria, or tissue and  
318 cellular preparations in which the barrier function of the plasma membrane is disrupted. Since  
319 this entails the loss of cell viability, mitochondrial preparations are not studied *in vivo*. In  
320 contrast to isolated mitochondria and tissue homogenate preparations, mitochondria in  
321 permeabilized tissues and cells are *in situ* relative to the plasma membrane. The plasma  
322 membrane separates the intracellular compartment including the cytosol, nucleus, and  
323 organelles from the environment of the cell. The plasma membrane consists of a lipid bilayer,  
324 embedded proteins, and attached organic molecules that collectively control the selective  
325 permeability of ions, organic molecules, and particles across the cell boundary. The intact  
326 plasma membrane prevents the passage of many water-soluble mitochondrial substrates and  
327 inorganic ions—such as succinate, adenosine diphosphate (ADP) and inorganic phosphate (P<sub>i</sub>),  
328 that must be controlled at kinetically-saturating concentrations for the analysis of respiratory  
329 capacities; this limits the scope of investigations into mitochondrial respiratory function in  
330 intact cells.

331 The cholesterol content of the plasma membrane is high compared to mitochondrial  
332 membranes. Therefore, mild detergents—such as digitonin and saponin—can be applied to  
333 selectively permeabilize the plasma membrane by interaction with cholesterol and allow free  
334 exchange of organic molecules and inorganic ions between the cytosol and the immediate cell  
335 environment, while maintaining the integrity and localization of organelles, cytoskeleton, and  
336 the nucleus. Application of optimum concentrations of permeabilization agents (mild detergents  
337 or toxins) leads to washout of cytosolic marker enzymes—such as lactate dehydrogenase—and  
338 results in the complete loss of cell viability, tested by nuclear staining using membrane-  
339 impermeable dyes, while mitochondrial function remains intact. Respiration of isolated  
340 mitochondria remains unaltered after the addition of low concentrations of digitonin or saponin.  
341 In addition to mechanical cell disruption during homogenization of tissue, permeabilization  
342 agents may be applied to ensure permeabilization of all cells. Suspensions of cells  
343 permeabilized in the respiration chamber and crude tissue homogenates contain all components  
344 of the cell at highly dilute concentrations. All mitochondria are retained in chemically-  
345 permeabilized mitochondrial preparations and crude tissue homogenates. In the preparation of  
346 isolated mitochondria, the cells or tissues are homogenized, and the mitochondria are separated  
347 from other cell fractions and purified by differential centrifugation, entailing the loss of a  
348 fraction of the total mitochondrial content. Typical mitochondrial recovery ranges from 30% to  
349 80%. Maximization of the purity of isolated mitochondria may compromise not only the  
350 mitochondrial yield but also the structural and functional integrity. Therefore, protocols to  
351 isolate mitochondria need to be optimized according to each study. The term mitochondrial  
352 preparation does not include further fractionation of mitochondrial components, neither  
353 submitochondrial particles.

354

### 355 2.1. Respiratory control and coupling

356

357 Respiratory coupling control states are established in studies of mitochondrial  
358 preparations to obtain reference values for various output variables. Physiological conditions *in*  
359 *vivo* deviate from these experimentally obtained states. Since kinetically-saturating  
360 concentrations, *e.g.*, of ADP or oxygen (O<sub>2</sub>; dioxygen), may not apply to physiological  
361 intracellular conditions, relevant information is obtained in studies of kinetic responses to  
362 variations in [ADP] or [O<sub>2</sub>] in the range between kinetically-saturating concentrations and  
363 anoxia (Gnaiger 2001).

364

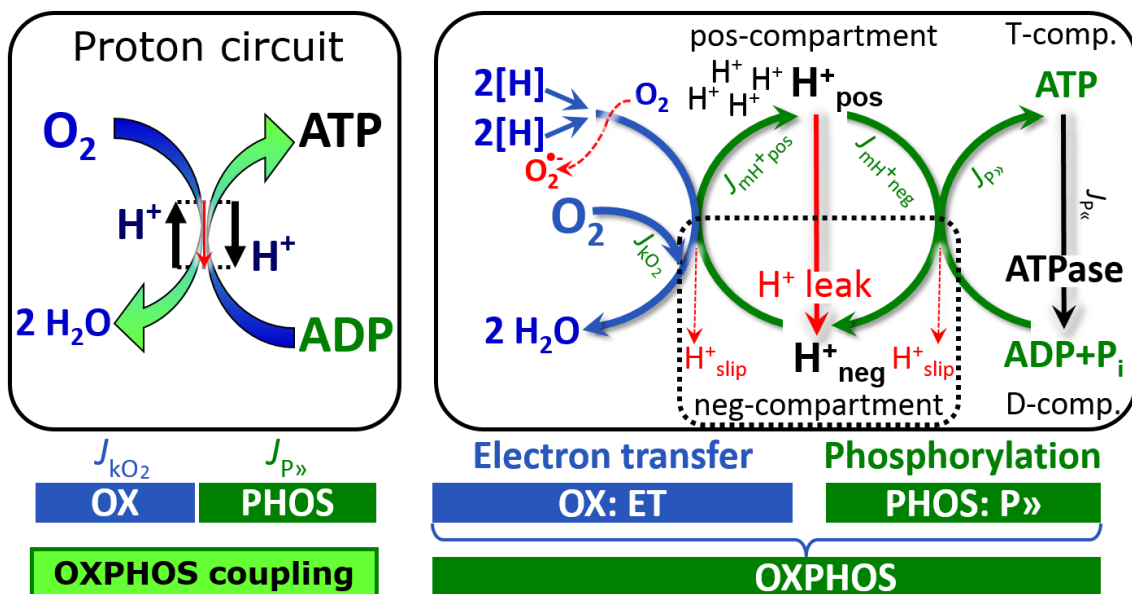
365 **The steady-state:** Mitochondria represent a thermodynamically open system in non-  
366 equilibrium states of biochemical energy transformation. State variables (protonmotive force;  
367 redox states) and metabolic *rates* (fluxes) are measured in defined mitochondrial respiratory  
368 *states*. Steady-states can be obtained only in open systems, in which changes by *internal*  
369 transformations, *e.g.*, O<sub>2</sub> consumption, are instantaneously compensated for by *external* fluxes,  
370 *e.g.*, O<sub>2</sub> supply, preventing a change of O<sub>2</sub> concentration in the system (Gnaiger 1993b).  
371 Mitochondrial respiratory states monitored in closed systems satisfy the criteria of pseudo-  
372 steady states for limited periods of time, when changes in the system (concentrations of O<sub>2</sub>, fuel  
373 substrates, ADP, P<sub>i</sub>, H<sup>+</sup>) do not exert significant effects on metabolic fluxes (respiration,  
374 phosphorylation). Such pseudo-steady states require respiratory media with sufficient buffering  
375 capacity and substrates maintained at kinetically-saturating concentrations, and thus depend on  
376 the kinetics of the processes under investigation.

376

377 **Specification of biochemical dose:** Substrates, uncouplers, inhibitors, and other  
378 biochemical reagents are titrated to dissect mitochondrial function. Nominal concentrations of  
379 these substances are usually reported as initial amount of substance concentration [mol·L<sup>-1</sup>] in  
380 the incubation medium. When aiming at the measurement of kinetically saturated processes—  
381 such as OXPHOS-capacities, the concentrations for substrates can be chosen according to the  
apparent equilibrium constant,  $K_m$ . In the case of hyperbolic kinetics, only 80% of maximum



382 respiratory capacity is obtained at a substrate concentration of four times the  $K_m'$ , whereas  
 383 substrate concentrations of 5, 9, 19 and 49 times the  $K_m'$  are theoretically required for reaching  
 384 83%, 90%, 95% or 98% of the maximal rate (Gnaiger 2001). Other reagents are chosen to  
 385 inhibit or alter some processes. The amount of these chemicals in an experimental incubation  
 386 is selected to maximize effect, avoiding unacceptable off-target consequences that would  
 387 adversely affect the data being sought. Specifying the amount of substance in an incubation as  
 388 nominal concentration in the aqueous incubation medium can be ambiguous (Doskey *et al.*  
 389 2015), particularly for lipophilic substances (oligomycin, uncouplers, permeabilization agents)  
 390 or cations (TPP<sup>+</sup>; fluorescent dyes such as safranin, TMRM), which accumulate in biological  
 391 membranes or in the mitochondrial matrix. For example, a dose of digitonin of 8 fmol·cell<sup>-1</sup> (10  
 392 pg·cell<sup>-1</sup>; 10 μg·10<sup>-6</sup> cells) is optimal for permeabilization of endothelial cells, and the  
 393 concentration in the incubation medium has to be adjusted according to the cell density applied  
 394 (Doerrier *et al.* 2018). Generally, dose/exposure can be specified per unit of biological sample,  
 395 *i.e.*, (nominal moles of xenobiotic)/(number of cells) [mol·cell<sup>-1</sup>] or, as appropriate, per mass of  
 396 biological sample [mol·kg<sup>-1</sup>]. This approach to specification of dose/exposure provides a  
 397 scalable parameter that can be used to design experiments, help interpret a wide variety of  
 398 experimental results, and provide absolute information that allows researchers worldwide to  
 399 make the most use of published data (Doskey *et al.* 2015).  
 400



401 **Fig. 2. The proton circuit and coupling in oxidative phosphorylation (OXPHOS).** 2[H]  
 402 indicates the reduced hydrogen equivalents of fuel substrates of the catabolic reaction k with  
 403 oxygen.  $O_2$  flux,  $J_{kO_2}$ , through the catabolic ET-pathway, is coupled to flux through the  
 404 phosphorylation-pathway of ADP to ATP,  $J_{P\gg}$ . The proton pumps of the ET-pathway drive  
 405 proton flux into the positive (pos) compartment,  $J_{mH^+pos}$ , generating the output protonmotive  
 406 force (motive, subscript m). F-ATPase is coupled to inward proton current into the negative  
 407 (neg) compartment,  $J_{mH^+neg}$ , to phosphorylate  $ADP+P_i$  to ATP. The system defined by the  
 408 boundaries (full black line) is not a black box, but is analysed as a compartmental system. The  
 409 negative compartment (neg-compartment, enclosed by the dotted line) is the matrix space,  
 410 separated by the mtIM from the positive compartment (pos-compartment).  $ADP+P_i$  and ATP  
 411 are the substrate- and product-compartments (scalar ADP and ATP compartments, D-comp.  
 412 and T-comp.), respectively. At steady-state proton turnover,  $J_{\infty H^+}$ , and ATP turnover,  $J_{\infty P}$ ,  
 413 maintain concentrations constant, when  $J_{mH^+\infty} = J_{mH^+pos} = J_{mH^+neg}$ , and  $J_{P\gg} = J_{P\gg} = J_{P\ll}$ . Modified  
 414 from Gnaiger (2014).  
 415  
 416

417 **Phosphorylation, P $\gg$ , and P $\gg$ /O $_2$  ratio:** *Phosphorylation* in the context of OXPHOS is  
 418 defined as phosphorylation of ADP by P $_i$  to form ATP. On the other hand, the term  
 419 phosphorylation is used generally in many contexts, *e.g.*, protein phosphorylation. This justifies  
 420 consideration of a symbol more discriminating and specific than P as used in the P/O ratio  
 421 (phosphate to atomic oxygen ratio), where P indicates phosphorylation of ADP to ATP or GDP  
 422 to GTP. We propose the symbol P $\gg$  for the endergonic (uphill) direction of phosphorylation  
 423 ADP $\rightarrow$ ATP, and likewise the symbol P $\ll$  for the corresponding exergonic (downhill) hydrolysis  
 424 ATP $\rightarrow$ ADP (**Fig. 2**). P $\gg$  refers mainly to electrontransfer phosphorylation but may also involve  
 425 substrate-level phosphorylation as part of the tricarboxylic acid (TCA) cycle (succinyl-CoA  
 426 ligase; phosphoglycerate kinase) and phosphorylation of ADP catalyzed by pyruvate kinase,  
 427 and of GDP phosphorylated by phosphoenolpyruvate carboxykinase. Transphosphorylation is  
 428 performed by adenylate kinase, creatine kinase, hexokinase and nucleoside diphosphate kinase.  
 429 In isolated mammalian mitochondria, ATP production catalyzed by adenylate kinase (2 ADP  
 430  $\leftrightarrow$  ATP + AMP) proceeds without fuel substrates in the presence of ADP (Komlódi and Tretter  
 431 2017). Kinase cycles are involved in intracellular energy transfer and signal transduction for  
 432 regulation of energy flux.

433 The P $\gg$ /O $_2$  ratio (P $\gg$ /4 e $^-$ ) is two times the ‘P/O’ ratio (P $\gg$ /2 e $^-$ ) of classical bioenergetics.  
 434 P $\gg$ /O $_2$  is a generalized symbol, not specific for determination of P $_i$  consumption (P $_i$ /O $_2$  flux  
 435 ratio), ADP depletion (ADP/O $_2$  flux ratio), or ATP production (ATP/O $_2$  flux ratio). The  
 436 mechanistic P $\gg$ /O $_2$  ratio—or P $\gg$ /O $_2$  stoichiometry—is calculated from the proton-to-O $_2$  and  
 437 proton-to-phosphorylation coupling stoichiometries (**Fig. 1A**):

$$438 \quad 439 \quad P\gg/O_2 = \frac{H_{\text{pos}}^+/O_2}{H_{\text{neg}}^+/P\gg} \quad (1)$$

440  
 441 The H $^+$ <sub>pos</sub>/O $_2$  *coupling stoichiometry* (referring to the full 4 electron reduction of O $_2$ ) depends  
 442 on the ET-pathway control state which defines the relative involvement of the three coupling  
 443 sites (CI, CIII and CIV) in the catabolic pathway of electrons to O $_2$ . This varies with: (1) a  
 444 bypass of CI by single or multiple electron input into the Q-junction; and (2) a bypass of CIV  
 445 by involvement of alternative oxidases, AOX, which are not expressed in mammalian  
 446 mitochondria. H $^+$ <sub>pos</sub>/O $_2$  is 12 in the ET-pathways involving CIII and CIV as proton pumps,  
 447 increasing to 20 for the NADH-pathway (**Fig. 1A**), but a general consensus on H $^+$ <sub>pos</sub>/O $_2$   
 448 stoichiometries remains to be reached (Hinkle 2005; Wikström and Hummer 2012; Sazanov  
 449 2015). The H $^+$ <sub>neg</sub>/P $\gg$  coupling stoichiometry (3.7; **Fig. 1A**) is the sum of 2.7 H $^+$ <sub>neg</sub> required by  
 450 the F-ATPase of vertebrate and most invertebrate species (Watt *et al.* 2010) and the proton  
 451 balance in the translocation of ADP, ATP and P $_i$  (**Fig. 1B**). Taken together, the mechanistic  
 452 P $\gg$ /O $_2$  ratio is calculated at 5.4 and 3.3 for NADH- and succinate-linked respiration, respectively  
 453 (Eq. 1). The corresponding classical P $\gg$ /O ratios (referring to the 2 electron reduction of 0.5 O $_2$ )  
 454 are 2.7 and 1.6 (Watt *et al.* 2010), in agreement with the measured P $\gg$ /O ratio for succinate of  
 455  $1.58 \pm 0.02$  (Gnaiger *et al.* 2000).

456 The effective P $\gg$ /O $_2$  flux ratio ( $Y_{P\gg/O_2} = J_{P\gg}/J_{kO_2}$ ) is diminished relative to the mechanistic  
 457 P $\gg$ /O $_2$  ratio by intrinsic and extrinsic uncoupling and dyscoupling (**Fig. 3**). Such generalized  
 458 uncoupling is different from switching to mitochondrial pathways that involve fewer than three  
 459 proton pumps (‘coupling sites’: Complexes CI, CIII and CIV), bypassing CI through multiple  
 460 electron entries into the Q-junction, or CIII and CIV through AOX (**Fig. 1**). Reprogramming of  
 461 mitochondrial pathways may be considered as a switch of gears (changing the stoichiometry)  
 462 rather than uncoupling (loosening the stoichiometry). In addition,  $Y_{P\gg/O_2}$  depends on several  
 463 experimental conditions of flux control, increasing as a hyperbolic function of [ADP] to a  
 464 maximum value (Gnaiger 2001).

465 **Control and regulation:** The terms metabolic *control* and *regulation* are frequently used  
 466 synonymously, but are distinguished in metabolic control analysis: ‘We could understand the

467 regulation as the mechanism that occurs when a system maintains some variable constant over  
 468 time, in spite of fluctuations in external conditions (homeostasis of the internal state). On the  
 469 other hand, metabolic control is the power to change the state of the metabolism in response to  
 470 an external signal' (Fell 1997). Respiratory control may be induced by experimental control  
 471 signals that *exert* an influence on: (1) ATP demand and ADP phosphorylation-rate; (2) fuel  
 472 substrate composition, pathway competition; (3) available amounts of substrates and O<sub>2</sub>, *e.g.*,  
 473 starvation and hypoxia; (4) the protonmotive force, redox states, flux–force relationships,  
 474 coupling and efficiency; (5) Ca<sup>2+</sup> and other ions including H<sup>+</sup>; (6) inhibitors, *e.g.*, nitric oxide  
 475 or intermediary metabolites such as oxaloacetate; (7) signalling pathways and regulatory  
 476 proteins, *e.g.*, insulin resistance, transcription factor hypoxia inducible factor 1. *Mechanisms* of  
 477 respiratory control and regulation include adjustments of: (1) enzyme activities by allosteric  
 478 mechanisms and phosphorylation; (2) enzyme content, concentrations of cofactors and  
 479 conserved moieties—such as adenylates, nicotinamide adenine dinucleotide [NAD<sup>+</sup>/NADH],  
 480 coenzyme Q, cytochrome *c*); (3) metabolic channeling by supercomplexes; and (4)  
 481 mitochondrial density (enzyme concentrations and membrane area) and morphology (cristae  
 482 folding, fission and fusion). Mitochondria are targeted directly by hormones, thereby affecting  
 483 their energy metabolism (Lee *et al.* 2013; Gerö and Szabo 2016; Price and Dai 2016; Moreno  
 484 *et al.* 2017). Evolutionary or acquired differences in the genetic and epigenetic basis of  
 485 mitochondrial function (or dysfunction) between subjects and gene therapy; age; gender,  
 486 biological sex, and hormone concentrations; life style including exercise and nutrition; and  
 487 environmental issues including thermal, atmospheric, toxicological and pharmacological  
 488 factors, exert an influence on all control mechanisms listed above. For reviews, see Brown  
 489 1992; Gnaiger 1993a, 2009; 2014; Paradies *et al.* 2014; Morrow *et al.* 2017.

490 **Respiratory control and response:** Lack of control by a metabolic pathway, *e.g.*,  
 491 phosphorylation-pathway, means that there will be no response to a variable activating it, *e.g.*,  
 492 [ADP]. The reverse, however, is not true as the absence of a response to [ADP] does not exclude  
 493 the phosphorylation-pathway from having some degree of control. The degree of control of a  
 494 component of the OXPHOS-pathway on an output variable—such as O<sub>2</sub> flux, will in general  
 495 be different from the degree of control on other outputs—such as phosphorylation-flux or  
 496 proton leak flux. Therefore, it is necessary to be specific as to which input and output are under  
 497 consideration (Fell 1997).

498 **Respiratory coupling control and ET-pathway control:** Respiratory control refers to  
 499 the ability of mitochondria to adjust O<sub>2</sub> flux in response to external control signals by engaging  
 500 various mechanisms of control and regulation. Respiratory control is monitored in a  
 501 mitochondrial preparation under conditions defined as respiratory states. When  
 502 phosphorylation of ADP to ATP is stimulated or depressed, an increase or decrease is observed  
 503 in electron flux linked to O<sub>2</sub> flux in respiratory coupling states of intact mitochondria  
 504 ('controlled states' in the classical terminology of bioenergetics). Alternatively, coupling of  
 505 electron transfer with phosphorylation is disengaged by disruption of the integrity of the mtIM  
 506 or by uncouplers, functioning like a clutch in a mechanical system. The corresponding coupling  
 507 control state is characterized by high levels of O<sub>2</sub> consumption without control by P»  
 508 ('uncontrolled state').

509 ET-pathway control states are obtained in mitochondrial preparations by depletion of  
 510 endogenous substrates and addition to the mitochondrial respiration medium of fuel substrates  
 511 (CHNO; 2[H] in **Fig. 2**) and specific inhibitors, activating selected mitochondrial catabolic  
 512 pathways, *k* (**Fig. 1**). Coupling control states and pathway control states are complementary,  
 513 since mitochondrial preparations depend on an exogenous supply of pathway-specific fuel  
 514 substrates and oxygen (Gnaiger 2014).

515 **Coupling:** In mitochondrial electron transfer (**Fig. 1**), vectorial transmembrane proton  
 516 flux is coupled through the proton pumps CI, CIII and CIV to the catabolic flux of scalar  
 517 reactions, collectively measured as O<sub>2</sub> flux (**Fig. 2**). Thus mitochondria are elements of energy

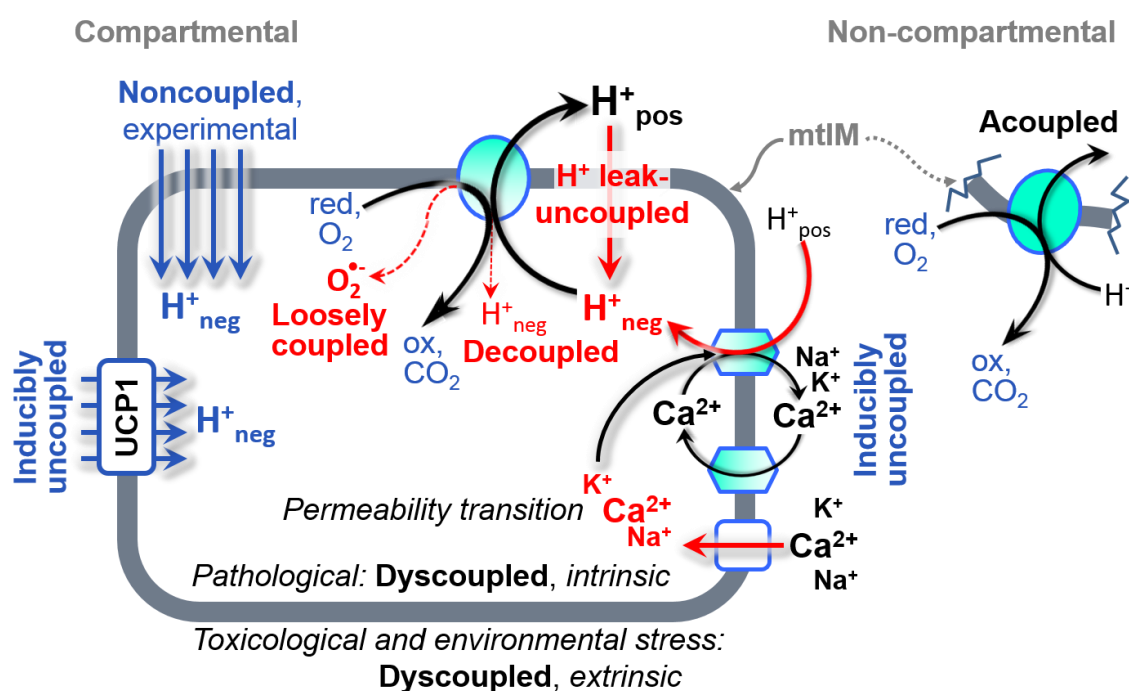
518 transformation. Energy cannot be lost or produced in any internal process (First Law of  
 519 thermodynamics). Open and closed systems can gain or lose energy only by external fluxes—  
 520 by exchange with the environment. Energy is a conserved quantity. Therefore, energy can  
 521 neither be produced by mitochondria, nor is there any internal process without energy  
 522 conservation. Exergy is defined as the ‘free energy’ with the potential to perform work.  
 523 *Coupling* is the mechanistic linkage of an exergonic process (spontaneous, negative exergy  
 524 change) with an endergonic process (positive exergy change) in energy transformations which  
 525 conserve part of the exergy that would be irreversibly lost or dissipated in an uncoupled process.

526 **Uncoupling:** Uncoupling of mitochondrial respiration is a general term comprising  
 527 diverse mechanisms:

- 528 1. Proton leak across the mtIM from the pos- to the neg-compartment (**Fig. 2**);
- 529 2. Cycling of other cations, strongly stimulated by permeability transition;
- 530 3. Proton slip in the proton pumps when protons are effectively not pumped (CI, CIII and  
 531 CIV) or are not driving phosphorylation (F-ATPase);
- 532 4. Loss of compartmental integrity when electron transfer is acoupled;
- 533 5. Electron leak in the loosely coupled univalent reduction of  $O_2$  to superoxide ( $O_2^{\cdot-}$ ;  
 534 superoxide anion radical).

535 Differences of terms—uncoupled vs. noncoupled—are easily overlooked, although they relate  
 536 to different meanings of uncoupling (**Fig. 3**).

537



538

539 **Fig 3. Mechanisms of respiratory uncoupling.** An intact mitochondrial inner membrane,  
 540 mtIM, is required for vectorial, compartmental coupling. ‘Acoupled’ respiration is the  
 541 consequence of structural disruption with catalytic activity of non-compartmental  
 542 mitochondrial fragments. Inducibly uncoupled (activation of UCP1) and experimentally  
 543 noncoupled respiration (titration of protonophores) stimulate respiration to maximum  $O_2$  flux.  
 544  $H^+$  leak-uncoupled, decoupled, and loosely coupled respiration are components of intrinsic  
 545 uncoupling. Pathological dysfunction may affect all types of uncoupling, including  
 546 permeability transition, causing intrinsically dyscoupled respiration. Similarly, toxicological  
 547 and environmental stress factors can cause extrinsically dyscoupled respiration.

548

549

550



## 551 2.2. Coupling states and respiratory rates

552

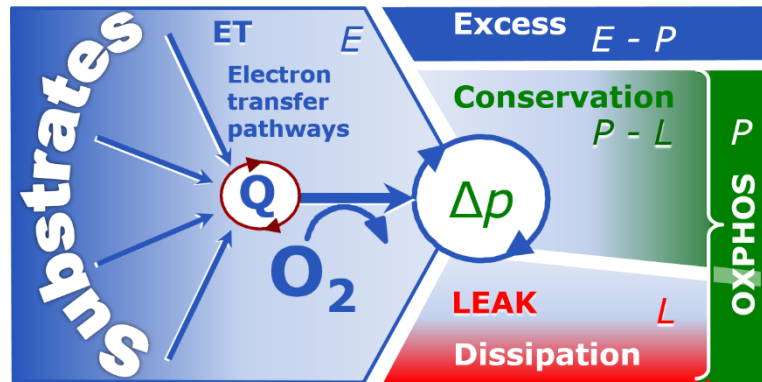
553 **Respiratory capacities in coupling control states:** To extend the classical nomenclature  
 554 on mitochondrial coupling states (Section 2.3) by a concept-driven terminology that  
 555 incorporates explicitly information on the nature of respiratory states, the terminology must be  
 556 general and not restricted to any particular experimental protocol or mitochondrial preparation  
 557 (Gnaiger 2009). We focus primarily on the conceptual ‘why’, along with clarification of the  
 558 experimental ‘how’. Respiratory capacities delineate, comparable to channel capacity in  
 559 information theory (Schneider 2006), the upper bound of the rate of respiration measured in  
 560 defined coupling control states and electron transfer-pathway (ET-pathway) states (**Fig. 4**).

561

562 **Fig. 4. Four-compartment model of oxidative phosphorylation.**

563 Respiratory states (ET, OXPHOS, LEAK; **Table 1**) and corresponding rates ( $E$ ,  $P$ ,  $L$ ) are connected by the  
 564 protonmotive force,  $\Delta p$ . ET-capacity,  $E$ , is partitioned into (1) dissipative LEAK-respiration,  $L$ ,  
 565 when the Gibbs energy change of catabolic  $O_2$  flux is irreversibly  
 566 lost, (2) net OXPHOS-capacity,  $P-L$ , with partial conservation of the capacity to perform work,  
 567 and (3) the excess capacity,  $E-P$ . Modified from Gnaiger (2014).

568  
 569  
 570  
 571  
 572  
 573  
 574  
 575



576 **Table 1. Coupling states and residual oxygen consumption in mitochondrial**  
 577 **preparations in relation to respiration- and phosphorylation-flux,  $J_{kO_2}$  and  $J_{P_{\gg}}$ ,**  
 578 **and protonmotive force,  $\Delta p$ .** Coupling states are established at kinetically-saturating  
 579 concentrations of fuel substrates and  $O_2$ .

State	$J_{kO_2}$	$J_{P_{\gg}}$	$\Delta p$	Inducing factors	Limiting factors
LEAK	$L$ ; low, cation leak-dependent respiration	0	max.	proton leak, slip, and cation cycling	$J_{P_{\gg}} = 0$ : (1) without ADP, $L_N$ ; (2) max. ATP/ADP ratio, $L_T$ ; or (3) inhibition of the phosphorylation-pathway, $L_{Omy}$
OXPHOS	$P$ ; high, ADP-stimulated respiration	max.	high	kinetically-saturating [ADP] and $[P_i]$	$J_{P_{\gg}}$ by phosphorylation-pathway; or $J_{kO_2}$ by ET-capacity
ET	$E$ ; max., noncoupled respiration	0	low	optimal external uncoupler concentration for max. $J_{O_2,E}$	$J_{kO_2}$ by ET-capacity
ROX	$R_{ox}$ ; min., residual $O_2$ consumption	0	0	$J_{O_2,Rox}$ in non-ET-pathway oxidation reactions	full inhibition of ET-pathway; or absence of fuel substrates

580

581 To provide a diagnostic reference for respiratory capacities of core energy metabolism,  
 582 the capacity of *oxidative phosphorylation*, OXPHOS, is measured at kinetically-saturating  
 583 concentrations of ADP and  $P_i$ . The *oxidative* ET-capacity reveals the limitation of OXPHOS-  
 584 capacity mediated by the *phosphorylation*-pathway. The ET- and phosphorylation-pathways  
 585 comprise coupled segments of the OXPHOS-system. ET-capacity is measured as noncoupled  
 586 respiration by application of *external uncouplers*. The contribution of *intrinsically uncoupled*  
 587  $O_2$  consumption is studied in the absence of ADP, by not stimulating phosphorylation, or by  
 588 inhibition of the phosphorylation-pathway. The corresponding states are collectively classified  
 589 as LEAK-states, when  $O_2$  consumption compensates mainly for ion leaks, including the proton  
 590 leak. Defined coupling states are induced by: (1) adding cation chelators such as EGTA, binding  
 591 free  $Ca^{2+}$  and thus limiting cation cycling; (2) adding ADP and  $P_i$ ; (3) inhibiting the  
 592 phosphorylation-pathway; and (4) uncoupler titrations, while maintaining a defined ET-  
 593 pathway state with constant fuel substrates and inhibitors of specific branches of the ET-  
 594 pathway (**Fig. 1**).

595 The three coupling states, ET, LEAK and OXPHOS, are shown schematically with the  
 596 corresponding respiratory rates, abbreviated as  $E$ ,  $L$  and  $P$ , respectively (**Fig. 4**). We distinguish  
 597 metabolic *pathways* from metabolic *states* and the corresponding metabolic *rates*; for example:  
 598 ET-pathways (**Fig. 4**), ET-state (**Fig. 5C**), and ET-capacity,  $E$ , respectively (**Table 1**). The  
 599 protonmotive force is *high* in the OXPHOS-state when it drives phosphorylation, *maximum* in  
 600 the LEAK-state of coupled mitochondria, driven by LEAK-respiration at a minimum back flux  
 601 of cations to the matrix side, and *very low* in the ET-state when uncouplers short-circuit the  
 602 proton cycle (**Table 1**).

603  $E$  may exceed or be equal to  $P$ .  $E > P$  is observed in many types of mitochondria, varying  
 604 between species, tissues and cell types (Gnaiger 2009).  $E - P$  is the excess ET-capacity pushing  
 605 the phosphorylation-flux (**Fig. 1B**) to the limit of its *capacity of utilizing* the protonmotive force.  
 606 In addition, the magnitude of  $E - P$  depends on the tightness of respiratory coupling or degree of  
 607 uncoupling, since an increase of  $L$  causes  $P$  to increase towards the limit of  $E$ . The *excess*  $E - P$   
 608 capacity,  $E - P$ , therefore, provides a sensitive diagnostic indicator of specific injuries of the  
 609 phosphorylation-pathway, under conditions when  $E$  remains constant but  $P$  declines relative to  
 610 controls (**Fig. 4**). Substrate cocktails supporting simultaneous convergent electron transfer to  
 611 the Q-junction for reconstitution of TCA cycle function establish pathway control states with  
 612 high ET-capacity, and consequently increase the sensitivity of the  $E - P$  assay.

613  $E$  cannot theoretically be lower than  $P$ .  $E < P$  must be discounted as an artefact, which  
 614 may be caused experimentally by: (1) loss of oxidative capacity during the time course of the  
 615 respirometric assay, since  $E$  is measured subsequently to  $P$ ; (2) using insufficient uncoupler  
 616 concentrations; (3) using high uncoupler concentrations which inhibit ET (Gnaiger 2008); (4)  
 617 high oligomycin concentrations applied for measurement of  $L$  before titrations of uncoupler,  
 618 when oligomycin exerts an inhibitory effect on  $E$ . On the other hand, the excess ET-capacity is  
 619 overestimated if non-saturating  $[ADP]$  or  $[P_i]$  are used. See State 3 in the next section.

620 The net OXPHOS-capacity is calculated by subtracting  $L$  from  $P$  (**Fig. 4**). Then the net  
 621  $P \gg O_2$  equals  $P \gg (P - L)$ , wherein the dissipative LEAK component in the OXPHOS-state may  
 622 be overestimated. This can be avoided by measuring LEAK-respiration in a state when the  
 623 protonmotive force is adjusted to its slightly lower value in the OXPHOS-state—by titration of  
 624 an ET inhibitor (Divakaruni and Brand 2011). Any turnover-dependent components of proton  
 625 leak and slip, however, are underestimated under these conditions (Garlid *et al.* 1993). In  
 626 general, it is inappropriate to use the term *ATP production* or *ATP turnover* for the difference  
 627 of  $O_2$  flux measured in states  $P$  and  $L$ . The difference  $P - L$  is the upper limit of the part of  
 628 OXPHOS-capacity that is freely available for ATP production (corrected for LEAK-  
 629 respiration) and is fully coupled to phosphorylation with a maximum mechanistic stoichiometry  
 630 (**Fig. 4**).



631 **LEAK-state (Fig. 5A):**  
 632 The LEAK-state is defined as a  
 633 state of mitochondrial respiration  
 634 when  $O_2$  flux mainly  
 635 compensates for ion leaks in the  
 636 absence of ATP synthesis, at  
 637 kinetically-saturating  
 638 concentrations of  $O_2$  and  
 639 respiratory fuel substrates.  
 640 LEAK-respiration is measured to  
 641 obtain an estimate of *intrinsic*  
 642 *uncoupling* without addition of  
 643 an experimental uncoupler: (1) in  
 644 the absence of adenylates; (2)  
 645 after depletion of ADP at a  
 646 maximum ATP/ADP ratio; or (3)  
 647 after inhibition of the  
 648 phosphorylation-pathway by  
 649 inhibitors of F-ATPase—such as  
 650 oligomycin, or of adenine  
 651 nucleotide translocase—such as  
 652 carboxyatractyloside.  
 653 Adjustment of the nominal  
 654 concentration of these inhibitors  
 655 to the density of biological  
 656 sample applied can minimize or  
 657 avoid inhibitory side-effects  
 658 exerted on ET-capacity or even  
 659 some dyscoupling.

661 **Proton leak and**  
 662 **uncoupled respiration:** Proton  
 663 leak is a leak current of protons.  
 664 The intrinsic proton leak is the  
 665 *uncoupled* process in which  
 666 protons diffuse across the mtIM  
 667 in the dissipative direction of the  
 668 downhill protonmotive force  
 669 without coupling to  
 670 phosphorylation (Fig. 5A). The  
 671 proton leak flux depends non-  
 672 linearly on the protonmotive  
 673 force (Garlid *et al.* 1989; Divakaruni and Brand 2011), it is a property of the mtIM and may be  
 674 enhanced due to possible contaminations by free fatty acids. Inducible uncoupling mediated by  
 675 uncoupling protein 1 (UCP1) is physiologically controlled, *e.g.*, in brown adipose tissue. UCP1  
 676 is a member of the mitochondrial carrier family which is involved in the translocation of protons  
 677 across the mtIM (Klingenberg 2017). Consequently, the short-circuit diminishes the  
 678 protonmotive force and stimulates electron transfer to  $O_2$  and heat dissipation without  
 679 phosphorylation of ADP.

680 **Cation cycling:** There can be other cation contributors to leak current including calcium  
 681 and probably magnesium. Calcium current is balanced by mitochondrial  $Na^+/Ca^{2+}$  exchange,

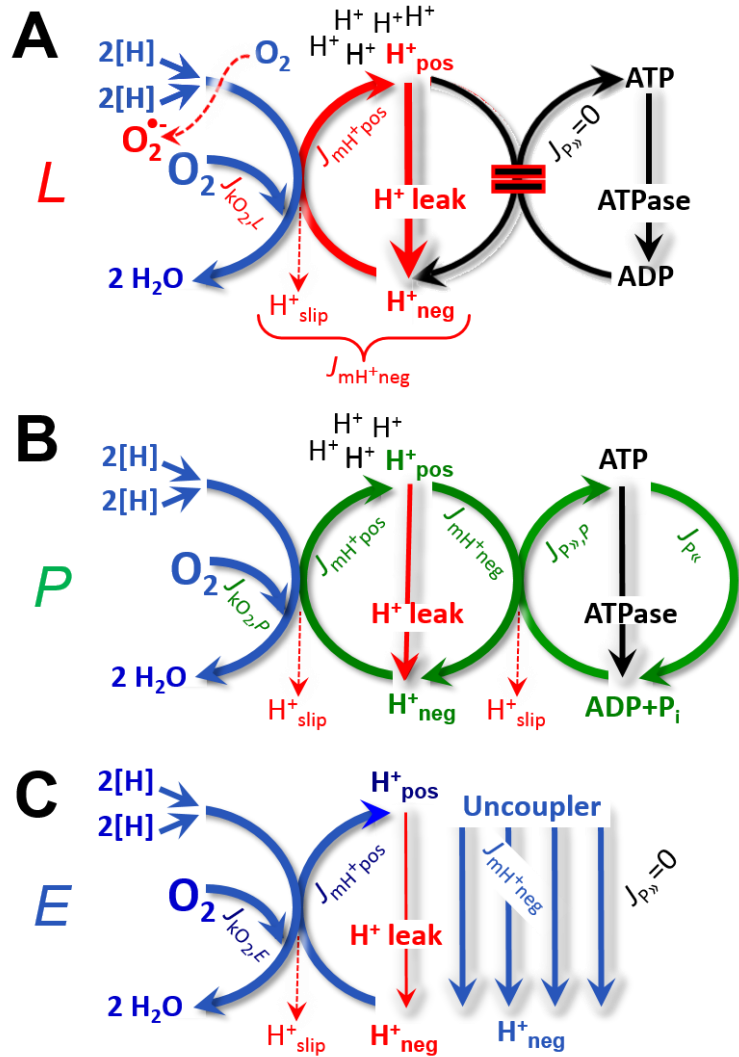



**Fig. 5. Respiratory coupling states. A: LEAK-state and rate, L:** Phosphorylation is arrested,  $J_{P_{\gg}} = 0$ , and catabolic  $O_2$  flux,  $J_{KO_2,L}$ , is controlled mainly by the proton leak,  $J_{mH^{+neg,L}}$ , at maximum protonmotive force (Fig. 3). **B: OXPHOS-state and rate, P:** Phosphorylation,  $J_{P_{\gg}}$ , is stimulated by kinetically-saturating [ADP] and  $[P_i]$ , and is supported by a high protonmotive force.  $O_2$  flux,  $J_{KO_2,P}$ , is well-coupled at a  $P_{\gg}/O_2$  ratio of  $J_{P_{\gg},P}/J_{KO_2,P}$ . **C: ET-state and rate, E:** Noncoupled respiration,  $J_{KO_2,E}$ , is maximum at optimum exogenous uncoupler concentration and phosphorylation is zero,  $J_{P_{\gg}} = 0$ . See also Fig. 2.

682 which is balanced by  $\text{Na}^+/\text{H}^+$  or  $\text{K}^+/\text{H}^+$  exchanges. This is another effective uncoupling  
683 mechanism different from proton leak (**Table 2**).

684 **Proton slip and decoupled respiration:** Proton slip is the *decoupled* process in which  
685 protons are only partially translocated by a proton pump of the ET-pathways and slip back to  
686 the original compartment. The proton leak is the dominant contributor to the overall leak current  
687 in mammalian mitochondria incubated under physiological conditions at 37 °C, whereas proton  
688 slip is increased at lower experimental temperature (Canton *et al.* 1995). Proton slip can also  
689 happen in association with the F-ATPase, in which the proton slips downhill across the pump  
690 to the matrix without contributing to ATP synthesis. In each case, proton slip is a property of  
691 the proton pump and increases with the pump turnover rate.

692 **Electron leak and loosely coupled respiration:** Superoxide production by the ETS leads  
693 to a bypass of proton pumps and correspondingly lower  $\text{P}\gg/\text{O}_2$  ratio. This depends on the actual  
694 site of electron leak and the scavenging of hydrogen peroxide by cytochrome *c*, whereby  
695 electrons may re-enter the ETS with proton translocation by CIV.  
696

697 **Table 2. Terms on respiratory coupling and uncoupling.**

Term	$J_{\text{kO}_2}$	$\text{P}\gg/\text{O}_2$	Note		
acoupled		0	electron transfer in mitochondrial fragments without vectorial proton translocation ( <b>Fig. 3</b> )		
intrinsic, no protonophore added		uncoupled	<i>L</i>	0	non-phosphorylating LEAK-respiration ( <b>Fig. 5A</b> )
		proton leak-uncoupled		0	component of <i>L</i> , $\text{H}^+$ diffusion across the mtIM ( <b>Fig. 3</b> )
		decoupled		0	component of <i>L</i> , proton slip ( <b>Fig. 3</b> )
		loosely coupled		0	component of <i>L</i> , lower coupling due to superoxide formation and bypass of proton pumps ( <b>Fig. 3</b> )
		dyscoupled		0	pathologically, toxicologically, environmentally increased uncoupling, mitochondrial dysfunction
		inducibly uncoupled		0	by UCP1 or cation ( <i>e.g.</i> , $\text{Ca}^{2+}$ ) cycling ( <b>Fig. 3</b> )
noncoupled	<i>E</i>	0	non-phosphorylating respiration stimulated to maximum flux at optimum exogenous uncoupler concentration ( <b>Fig. 5C</b> )		
well-coupled	<i>P</i>	high	phosphorylating respiration with an intrinsic LEAK component ( <b>Fig. 5B</b> )		
fully coupled	<i>P - L</i>	max.	OXPPOS-capacity corrected for LEAK-respiration ( <b>Fig. 4</b> )		

698 **Loss of compartmental integrity and acoupled respiration:** Electron transfer and  
699 catabolic  $\text{O}_2$  flux proceed without compartmental proton translocation in disrupted  
700 mitochondrial fragments. Such fragments form during mitochondrial isolation, and may not  
701 fully fuse to re-establish structurally intact mitochondria. Loss of mtIM integrity, therefore, is  
702 the cause of acoupled respiration, which is a nonvectorial dissipative process without control  
703 by the protonmotive force.  
704

705 **Dyscoupled respiration:** Mitochondrial injuries may lead to *dyscoupling* as a  
706 pathological or toxicological cause of *uncoupled* respiration. Dyscoupling may involve any  
707 type of uncoupling mechanism, *e.g.*, opening the permeability transition pore. Dyscoupled

708 respiration is distinguished from the experimentally induced *noncoupled* respiration in the ET-  
709 state (**Table 2**).

710 **OXPPOS-state (Fig. 5B):** The OXPPOS-state is defined as the respiratory state with  
711 kinetically-saturating concentrations of O<sub>2</sub>, respiratory and phosphorylation substrates, and  
712 absence of exogenous uncoupler, which provides an estimate of the maximal respiratory  
713 capacity in the OXPPOS-state for any given ET-pathway state. Respiratory capacities at  
714 kinetically-saturating substrate concentrations provide reference values or upper limits of  
715 performance, aiming at the generation of data sets for comparative purposes. Physiological  
716 activities and effects of substrate kinetics can be evaluated relative to the OXPPOS-capacity.

717 As discussed previously, 0.2 mM ADP does not fully saturate flux in isolated  
718 mitochondria (Gnaiger 2001; Puchowicz *et al.* 2004); greater ADP concentration is required,  
719 particularly in permeabilized muscle fibres and cardiomyocytes, to overcome limitations by  
720 intracellular diffusion and by the reduced conductance of the mtOM (Jepihhina *et al.* 2011,  
721 Illaste *et al.* 2012, Simson *et al.* 2016), either through interaction with tubulin (Rostovtseva *et al.*  
722 2008) or other intracellular structures (Birkedal *et al.* 2014). In permeabilized muscle fibre  
723 bundles of high respiratory capacity, the apparent  $K_m$  for ADP increases up to 0.5 mM (Saks *et al.*  
724 1998), consistent with experimental evidence that >90% saturation is reached only at >5  
725 mM ADP (Pesta and Gnaiger 2012). Similar ADP concentrations are also required for accurate  
726 determination of OXPPOS-capacity in human clinical cancer samples and permeabilized cells  
727 (Klepinin *et al.* 2016; Koit *et al.* 2017). Whereas 2.5 to 5 mM ADP is sufficient to obtain the  
728 actual OXPPOS-capacity in many types of permeabilized tissue and cell preparations,  
729 experimental validation is required in each specific case.

730 **Electron transfer-state (Fig. 5C):** The ET-state is defined as the *noncoupled* state with  
731 kinetically-saturating concentrations of O<sub>2</sub>, respiratory substrate and optimum *exogenous*  
732 uncoupler concentration for maximum O<sub>2</sub> flux. O<sub>2</sub> flux determined in the ET-state yields an  
733 estimate of ET-capacity. Inhibition of respiration is observed at higher than optimum uncoupler  
734 concentrations. As a consequence of the nearly collapsed protonmotive force, the driving force  
735 is insufficient for phosphorylation, and  $J_{P_s} = 0$ .

736 **ROX state and Rox:** Besides the three fundamental coupling states of mitochondrial  
737 preparations, the state of residual O<sub>2</sub> consumption, ROX, is relevant to assess respiratory  
738 function. ROX is not a coupling state. The rate of residual oxygen consumption, *Rox*, is defined  
739 as O<sub>2</sub> consumption due to oxidative side reactions measured after inhibition of ET—with  
740 rotenone, malonic acid and antimycin A. Cyanide and azide inhibit CIV and several peroxidases  
741 involved in *Rox*. ROX represents a baseline that is used to correct respiration in defined  
742 coupling states. *Rox* is not necessarily equivalent to non-mitochondrial respiration, considering  
743 O<sub>2</sub>-consuming reactions in mitochondria not related to ET—such as O<sub>2</sub> consumption in  
744 reactions catalyzed by monoamine oxidases (type A and B), monooxygenases (cytochrome  
745 P450 monooxygenases), dioxygenase (sulfur dioxygenase and trimethyllysine dioxygenase),  
746 and several hydroxylases. Mitochondrial preparations, especially those obtained from liver, may  
747 be contaminated by peroxisomes. This fact makes the exact determination of mitochondrial O<sub>2</sub>  
748 consumption and mitochondria-associated generation of reactive oxygen species complicated  
749 (Schönfeld *et al.* 2009). The dependence of ROX-linked O<sub>2</sub> consumption needs to be studied  
750 in detail together with non-ET enzyme activities, availability of specific substrates, O<sub>2</sub>  
751 concentration, and electron leakage leading to the formation of reactive oxygen species.

### 752 2.3. Classical terminology for isolated mitochondria

754 'When a code is familiar enough, it ceases appearing like a code; one forgets that there  
755 is a decoding mechanism. The message is identical with its meaning' (Hofstadter 1979).

756  
757 Chance and Williams (1955; 1956) introduced five classical states of mitochondrial  
758 respiration and cytochrome redox states. **Table 3** shows a protocol with isolated mitochondria

759 in a closed respirometric chamber, defining a sequence of respiratory states. States and rates  
760 are not specifically distinguished in this nomenclature.

761 **State 1** is obtained after addition of isolated mitochondria to air-saturated  
762 isoosmotic/isotonic respiration medium containing  $P_i$ , but no fuel substrates and no adenylates,  
763 *i.e.*, AMP, ADP, ATP.

764 **State 2** is induced by addition of a ‘high’ concentration of ADP (typically 100 to 300  
765  $\mu\text{M}$ ), which stimulates respiration transiently on the basis of endogenous fuel substrates and  
766 phosphorylates only a small portion of the added ADP. State 2 is then obtained at a low  
767 respiratory activity limited by exhausted endogenous fuel substrate availability (**Table 3**). If  
768 addition of specific inhibitors of respiratory complexes—such as rotenone—does not cause a  
769 further decline of  $\text{O}_2$  flux, State 2 is equivalent to the ROX state (See below.). If inhibition is  
770 observed, undefined endogenous fuel substrates are a confounding factor of pathway control,  
771 contributing to the effect of subsequently externally added substrates and inhibitors. In contrast  
772 to the original protocol, an alternative sequence of titration steps is frequently applied, in which  
773 the alternative ‘State 2’ has an entirely different meaning, when this second state is induced by  
774 addition of fuel substrate without ADP (LEAK-state; in contrast to State 2 defined in **Table 1**  
775 as a ROX state), followed by addition of ADP.

776  
777 **Table 3. Metabolic states of mitochondria (Chance and**  
778 **Williams, 1956; Table V).**

State	$[\text{O}_2]$	ADP level	Substrate level	Respiration rate	Rate-limiting substance
1	>0	low	low	slow	ADP
2	>0	high	~0	slow	substrate
3	>0	high	high	fast	respiratory chain
4	>0	low	high	slow	ADP
5	0	high	high	0	oxygen

780  
781 **State 3** is the state stimulated by addition of fuel substrates while the ADP concentration  
782 is still high (**Table 3**) and supports coupled energy transformation through oxidative  
783 phosphorylation. ‘High ADP’ is a concentration of ADP specifically selected to allow the  
784 measurement of State 3 to State 4 transitions of isolated mitochondria in a closed respirometric  
785 chamber. Repeated ADP titration re-establishes State 3 at ‘high ADP’. Starting at  $\text{O}_2$   
786 concentrations near air-saturation (ca. 200  $\mu\text{M}$   $\text{O}_2$  at sea level and 37 °C), the total ADP  
787 concentration added must be low enough (typically 100 to 300  $\mu\text{M}$ ) to allow phosphorylation  
788 to ATP at a coupled  $\text{O}_2$  flux that does not lead to  $\text{O}_2$  depletion during the transition to State 4.  
789 In contrast, kinetically-saturating ADP concentrations usually are 10-fold higher than ‘high  
790 ADP’, *e.g.*, 2.5 mM in isolated mitochondria. The abbreviation State 3u is occasionally used in  
791 bioenergetics, to indicate the state of respiration after titration of an uncoupler, without  
792 sufficient emphasis on the fundamental difference between OXPHOS-capacity (*well-coupled*  
793 with an *endogenous* uncoupled component) and ET-capacity (*noncoupled*).

794 **State 4** is a LEAK-state that is obtained only if the mitochondrial preparation is intact  
795 and well-coupled. Depletion of ADP by phosphorylation to ATP causes a decline of  $\text{O}_2$  flux in  
796 the transition from State 3 to State 4. Under the conditions of State 4, a maximum protonmotive  
797 force and high ATP/ADP ratio are maintained. The gradual decline of  $Y_{P\gg/\text{O}_2}$  towards  
798 diminishing  $[\text{ADP}]$  at State 4 must be taken into account for calculation of  $P\gg/\text{O}_2$  ratios (Gnaiger  
799 2001). State 4 respiration,  $L_T$  (**Table 1**), reflects intrinsic proton leak and ATP hydrolysis  
800 activity.  $\text{O}_2$  flux in State 4 is an overestimation of LEAK-respiration if the contaminating ATP  
801 hydrolysis activity recycles some ATP to ADP,  $J_{P\ll}$ , which stimulates respiration coupled to  
802 phosphorylation,  $J_{P\gg} > 0$ . This can be tested by inhibition of the phosphorylation-pathway using



803 oligomycin, ensuring that  $J_{P_s} = 0$  (State 4o). Alternatively, sequential ADP titrations re-  
 804 establish State 3, followed by State 3 to State 4 transitions while sufficient  $O_2$  is available.  
 805 Anoxia may be reached, however, before exhaustion of ADP (State 5).

806 **State 5** is the state after exhaustion of  $O_2$  in a closed respirometric chamber. Diffusion of  
 807  $O_2$  from the surroundings into the aqueous solution may be a confounding factor preventing  
 808 complete anoxia (Gnaiger 2001). Chance and Williams (1955) provide an alternative definition  
 809 of State 5, which gives it the different meaning of ROX versus anoxia: ‘State 5 may be obtained  
 810 by antimycin A treatment or by anaerobiosis’.

811 In **Table 3**, only States 3 and 4 (and ‘State 2’ in the alternative protocol: addition of fuel  
 812 substrates without ADP; not included in the table) are coupling control states, with the  
 813 restriction that  $O_2$  flux in State 3 may be limited kinetically by non-saturating ADP  
 814 concentrations (**Table 1**).

815  
816

### 817 3. Normalization: fluxes and flows

818

#### 819 3.1. Normalization: system or sample

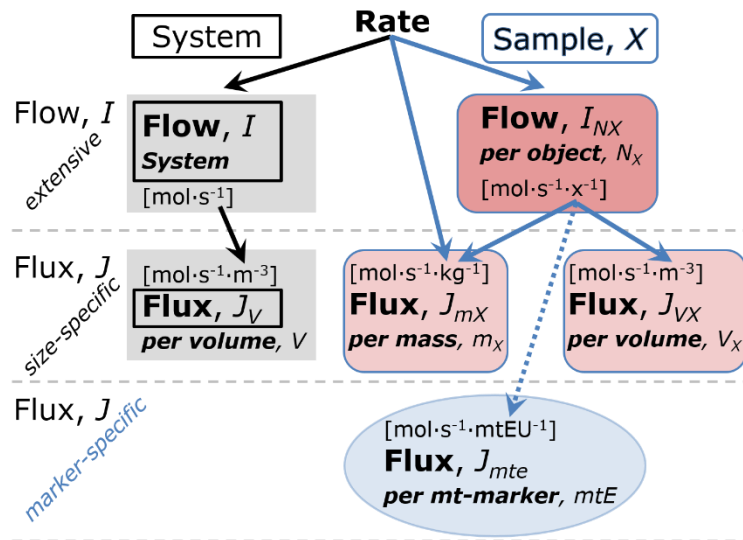
820

821 The term *rate* is not sufficiently defined to be useful for reporting data (**Fig. 6**). The  
 822 inconsistency of the meanings of rate becomes fully apparent when considering Galileo  
 823 Galilei’s famous principle, that ‘bodies of different weight all fall at the same rate (have a  
 824 constant acceleration)’ (Coopersmith 2010).

825

826 **Fig. 6. Different meanings of rate may lead to confusion, if the normalization is not**  
 827 **sufficiently specified.** Results are frequently expressed as mass-  
 828 specific *flux*,  $J_{mX}$ , per mg protein, dry or wet weight (mass). Cell  
 829 volume,  $V_{cell}$ , may be used for normalization (volume-specific  
 830 flux,  $J_{Vcell}$ ), which must be clearly distinguished from flow per cell,  
 831  $I_{Ncell}$ , or flux,  $J_V$ , expressed for methodological reasons per  
 832 volume of the measurement system. For details see **Table 4**.

841



### 842 Box 2: Metabolic fluxes and flows: vectorial and scalar

843

844 Fluxes are *vectors*, if they have *spatial* geometric direction in addition to magnitude.  
 845 Electric charge per unit time is electric flow or current,  $I_{el} = dQ_{el} \cdot dt^{-1}$  [A]. When expressed per  
 846 unit cross-sectional area,  $A$  [ $m^2$ ], a vector flux is obtained, which is current density or surface-  
 847 density of flow) perpendicular to the direction of flux,  $J_{el} = I_{el} \cdot A^{-1}$  [ $A \cdot m^{-2}$ ] (Cohen et al. 2008).  
 848 For all transformations *flows*,  $I_{tr}$ , are defined as extensive quantities. Vector and scalar *fluxes*  
 849 are obtained as  $J_{tr} = I_{tr} \cdot A^{-1}$  [ $mol \cdot s^{-1} \cdot m^{-2}$ ] and  $J_{tr} = I_{tr} \cdot V^{-1}$  [ $mol \cdot s^{-1} \cdot m^{-3}$ ], expressing flux as an area-  
 850 specific vector or volume-specific vectorial or scalar quantity, respectively (Gnaiger 1993b).

851 We suggest to define: (1) *vectorial* fluxes, which are translocations as functions of  
 852 *gradients* with direction in geometric space in continuous systems; (2) *vectorial* fluxes, which  
 853 describe translocations in discontinuous systems and are restricted to information on

854 *compartmental differences* (**Fig. 2**, transmembrane proton flux); and (3) *scalar* fluxes, which  
 855 are transformations in a *homogenous* system (**Fig. 2**, catabolic O<sub>2</sub> flux,  $J_{\text{KO}_2}$ ).

856 Vectorial transmembrane proton fluxes,  $J_{\text{mH}^+\text{pos}}$  and  $J_{\text{mH}^+\text{neg}}$ , are analyzed in a  
 857 heterogenous compartmental system as a quantity with *directional* but not *spatial* information.  
 858 Translocation of protons across the mtIM has a defined direction, either from the negative  
 859 compartment (matrix space; negative, neg-compartment) to the positive compartment (inter-  
 860 membrane space; positive, pos-compartment) or *vice versa* (**Fig. 2**). The arrows defining the  
 861 direction of the translocation between the two compartments may point upwards or downwards,  
 862 right or left, without any implication that these are actual directions in space. The pos-  
 863 compartment is neither above nor below the neg-compartment in a spatial sense, but can be  
 864 visualized arbitrarily in a figure in the upper position (**Fig. 2**). In general, the *compartmental*  
 865 *direction* of vectorial translocation from the neg-compartment to the pos-compartment is  
 866 defined by assigning the initial and final state as *ergodynamic compartments*,  $\text{H}^+_{\text{neg}} \rightarrow \text{H}^+_{\text{pos}}$  or  
 867  $0 = -1 \text{H}^+_{\text{neg}} + 1 \text{H}^+_{\text{pos}}$ , related to work (erg = work) that must be performed to lift the proton from  
 868 a lower to a higher electrochemical potential or from the lower to the higher ergodynamic  
 869 compartment (Gnaiger 1993b).

870 In analogy to *vectorial* translocation, the direction of a *scalar* chemical reaction,  $\text{A} \rightarrow \text{B}$   
 871 or  $0 = -1 \text{A} + 1 \text{B}$ , is defined by assigning substrates and products, A and B, as ergodynamic  
 872 compartments. O<sub>2</sub> is defined as a substrate in respiratory O<sub>2</sub> consumption, which together with  
 873 the fuel substrates comprises the substrate compartment of the catabolic reaction (**Fig. 2**).  
 874 Volume-specific scalar O<sub>2</sub> flux is coupled to vectorial translocation, yielding the  $\text{H}^+_{\text{pos}}/\text{O}_2$  ratio  
 875 (**Fig. 1**).

876

877

878 **Flow per system,  $I$ :** In a generalization of electrical terms, flow as an extensive quantity  
 879 ( $I$ ; per system) is distinguished from flux as a size-specific quantity ( $J$ ; per system size) (**Fig.**  
 880 **6**). Electric current is flow,  $I_{\text{el}}$  [ $\text{A} \equiv \text{C} \cdot \text{s}^{-1}$ ] per system (extensive quantity). When dividing this  
 881 extensive quantity by system size (cross-sectional area of a ‘wire’), a size-specific quantity is  
 882 obtained, which is flux (current density),  $J_{\text{el}}$  [ $\text{A} \cdot \text{m}^{-2} = \text{C} \cdot \text{s}^{-1} \cdot \text{m}^{-2}$ ].

883 **Extensive quantities:** An extensive quantity increases proportionally with system size.  
 884 The magnitude of an extensive quantity is completely additive for non-interacting  
 885 subsystems—such as mass or flow expressed per defined system. The magnitude of these  
 886 quantities depends on the extent or size of the system (Cohen *et al.* 2008).

887 **Size-specific quantities:** ‘The adjective *specific* before the name of an extensive quantity  
 888 is often used to mean *divided by mass*’ (Cohen *et al.* 2008). In this system-paradigm, mass-  
 889 specific flux is flow divided by mass of the *system* (the total mass of everything within the  
 890 measuring chamber or reactor). A mass-specific quantity is independent of the extent of non-  
 891 interacting homogenous subsystems. Tissue-specific quantities (related to the *sample* in  
 892 contrast to the *system*) are of fundamental interest in comparative mitochondrial physiology,  
 893 where *specific* refers to the *type of the sample* rather than *mass of the system*. The term *specific*,  
 894 therefore, must be clarified; *sample-specific*, e.g., muscle mass-specific normalization, is  
 895 distinguished from *system-specific* quantities (mass or volume; **Fig. 6**).

896

### 897 3.2. Normalization for system-size: flux per chamber volume

898

899 **System-specific flux,  $J_{V,\text{O}_2}$ :** The experimental system (experimental chamber) is part of  
 900 the measurement apparatus, separated from the environment as an isolated, closed, open,  
 901 isothermal or non-isothermal system (**Table 4**). On another level, we distinguish between (1)  
 902 the *system* with volume  $V$  and mass  $m$  defined by the system boundaries, and (2) the *sample* or  
 903 *objects* with volume  $V_X$  and mass  $m_X$  which are enclosed in the experimental chamber (**Fig. 6**).  
 904 Metabolic O<sub>2</sub> flow per object,  $I_{\text{O}_2/X}$ , increases as the mass of the object is increased. Sample



905 mass-specific O<sub>2</sub> flux,  $J_{O_2/mX}$  should be independent of the mass of the sample studied in the  
 906 instrument chamber, but system volume-specific O<sub>2</sub> flux,  $J_{V,O_2}$  (per volume of the instrument  
 907 chamber), should increase in direct proportion to the mass of the sample in the chamber.  
 908 Whereas  $J_{V,O_2}$  depends on mass-concentration of the sample in the chamber, it should be  
 909 independent of the chamber (system) volume at constant sample mass. There are practical  
 910 limitations to increase the mass-concentration of the sample in the chamber, when one is  
 911 concerned about crowding effects and instrumental time resolution.

912 When the reactor volume does not change during the reaction, which is typical for liquid  
 913 phase reactions, the volume-specific flux of a chemical reaction  $r$  is the time derivative of the  
 914 advancement of the reaction per unit volume,  $J_{V,rB} = d_r\zeta_B/dt \cdot V^{-1}$  [(mol·s<sup>-1</sup>)·L<sup>-1</sup>]. The rate of  
 915 concentration change is  $dc_B/dt$  [(mol·L<sup>-1</sup>)·s<sup>-1</sup>], where concentration is  $c_B = n_B/V$ . There is a  
 916 difference between (1)  $J_{V,rO_2}$  [mol·s<sup>-1</sup>·L<sup>-1</sup>] and (2) rate of concentration change [mol·L<sup>-1</sup>·s<sup>-1</sup>].  
 917 These merge to a single expression only in closed systems. In open systems, external fluxes  
 918 (such as O<sub>2</sub> supply) are distinguished from internal transformations (catabolic flux, O<sub>2</sub>  
 919 consumption). In a closed system, external flows of all substances are zero and O<sub>2</sub> consumption  
 920 (internal flow of catabolic reactions  $k$ ),  $I_{kO_2}$  [pmol·s<sup>-1</sup>], causes a decline of the amount of O<sub>2</sub> in  
 921 the system,  $n_{O_2}$  [nmol]. Normalization of these quantities for the volume of the system,  $V$  [L  $\equiv$   
 922 dm<sup>3</sup>], yields volume-specific O<sub>2</sub> flux,  $J_{V,kO_2} = I_{kO_2}/V$  [nmol·s<sup>-1</sup>·L<sup>-1</sup>], and O<sub>2</sub> concentration, [O<sub>2</sub>]  
 923 or  $c_{O_2} = n_{O_2}/V$  [ $\mu$ mol·L<sup>-1</sup> =  $\mu$ M = nmol·mL<sup>-1</sup>]. Instrumental background O<sub>2</sub> flux is due to external  
 924 flux into a non-ideal closed respirometer; then total volume-specific flux has to be corrected for  
 925 instrumental background O<sub>2</sub> flux—O<sub>2</sub> diffusion into or out of the instrumental chamber.  $J_{V,kO_2}$   
 926 is relevant mainly for methodological reasons and should be compared with the accuracy of  
 927 instrumental resolution of background-corrected flux, e.g.,  $\pm 1$  nmol·s<sup>-1</sup>·L<sup>-1</sup> (Gnaiger 2001).  
 928 ‘Metabolic’ or catabolic indicates O<sub>2</sub> flux,  $J_{kO_2}$ , corrected for: (1) instrumental background O<sub>2</sub>  
 929 flux; (2) chemical background O<sub>2</sub> flux due to autoxidation of chemical components added to  
 930 the incubation medium; and (3)  $R_{ox}$  for O<sub>2</sub>-consuming side reactions unrelated to the catabolic  
 931 pathway  $k$ .

932

### 933 3.3. Normalization: per sample

934

935 The challenges of measuring mitochondrial respiratory flux are matched by those of  
 936 normalization. Application of common and defined units is required for direct transfer of  
 937 reported results into a database. The second [s] is the SI unit for the base quantity *time*. It is also  
 938 the standard time-unit used in solution chemical kinetics. A rate may be considered as the  
 939 numerator and normalization as the complementary denominator, which are tightly linked in  
 940 reporting the measurements in a format commensurate with the requirements of a database.  
 941 Normalization (Table 4) is guided by physicochemical principles, methodological  
 942 considerations, and conceptual strategies (Fig. 7).

943 **Sample concentration,  $C_{mX}$ :** Normalization for sample concentration is required to  
 944 report respiratory data. Considering a tissue or cells as the sample,  $X$ , the sample mass is  $m_X$   
 945 [mg], which is frequently measured as wet or dry weight,  $W_w$  or  $W_d$  [mg], respectively, or as  
 946 amount of tissue or cell protein,  $m_{\text{Protein}}$ . In the case of permeabilized tissues, cells, and  
 947 homogenates, the sample concentration,  $C_{mX} = m_X/V$  [g·L<sup>-1</sup> = mg·mL<sup>-1</sup>], is the mass of the  
 948 subsample of tissue that is transferred into the instrument chamber.

949 **Mass-specific flux,  $J_{O_2/mX}$ :** Mass-specific flux is obtained by expressing respiration per  
 950 mass of sample,  $m_X$  [mg].  $X$  is the type of sample—isolated mitochondria, tissue homogenate,  
 951 permeabilized fibres or cells. Volume-specific flux is divided by mass concentration of  $X$ ,  $J_{O_2/mX}$   
 952 =  $J_{V,O_2}/C_{mX}$ ; or flow per cell is divided by mass per cell,  $J_{O_2/mcell} = I_{O_2/cell}/M_{cell}$ . If mass-specific  
 953 O<sub>2</sub> flux is constant and independent of sample size (expressed as mass), then there is no  
 954 interaction between the subsystems. A 1.5 mg and a 3.0 mg muscle sample respire at identical  
 955 mass-specific flux. Mass-specific O<sub>2</sub> flux, however, may change with the mass of a tissue

956 sample, cells or isolated mitochondria in the measuring chamber, in which the nature of the  
 957 interaction becomes an issue. Therefore, cell density must be optimized, particularly in  
 958 experiments carried out in wells, considering the confluency of the cell monolayer or clumps  
 959 of cells (Salabei *et al.* 2014).

960 **Number concentration,  $C_{NX}$ :**  $C_{NX}$  is the experimental *number concentration* of sample  
 961  $X$ . In the case of cells or animals, *e.g.*, nematodes,  $C_{NX} = N_X/V [X \cdot L^{-1}]$ , where  $N_X$  is the number  
 962 of cells or organisms in the chamber (**Table 4**).

963 **Flow per object,  $I_{O_2/X}$ :** A special case of normalization is encountered in respiratory  
 964 studies with permeabilized (or intact) cells. If respiration is expressed per cell, the  $O_2$  flow per  
 965 measurement system is replaced by the  $O_2$  flow per cell,  $I_{O_2/cell}$  (**Table 4**).  $O_2$  flow can be  
 966 calculated from volume-specific  $O_2$  flux,  $J_{V,O_2} [nmol \cdot s^{-1} \cdot L^{-1}]$  (per  $V$  of the measurement chamber  
 967 [L]), divided by the number concentration of cells,  $C_{N_{cell}} = N_{cell}/V [cell \cdot L^{-1}]$ , where  $N_{cell}$  is the  
 968 number of cells in the chamber. The total cell count is the sum of viable and dead cells,  $N_{cell} =$   
 969  $N_{vce} + N_{dce}$  (**Table 5**). The cell viability index,  $CVI = N_{vce}/N_{cell}$ , is the ratio of viable cells ( $N_{vce}$ ;  
 970 before experimental permeabilization) per total cell count. After experimental permeabilization,  
 971 all cells are permeabilized,  $N_{pce} = N_{cell}$ . The cell viability index can be used to normalize  
 972 respiration for the number of cells that have been viable before experimental permeabilization,  
 973  $I_{O_2/vce} = I_{O_2/cell}/CVI$ , considering that mitochondrial respiratory dysfunction in dead cells should  
 974 be eliminated as a confounding factor.

975

976

**Table 4. Sample concentrations and normalization of flux.**

Expression	Symbol	Definition	Unit	Notes
<b>Sample</b>				
identity of sample	$X$	object: cell, tissue, animal, patient		
number of sample entities $X$	$N_X$	number of objects	x	
mass of sample $X$	$m_X$		kg	1
mass of object $X$	$M_X$	$M_X = m_X \cdot N_X^{-1}$	kg · x <sup>-1</sup>	1
<b>Mitochondria</b>				
mitochondria	mt	$X = mt$		
amount of mt-elements	$mtE$	quantity of mt-marker	mtEU	
<b>Concentrations</b>				
object number concentration	$C_{NX}$	$C_{NX} = N_X \cdot V^{-1}$	x · m <sup>-3</sup>	2
sample mass concentration	$C_{mX}$	$C_{mX} = m_X \cdot V^{-1}$	kg · m <sup>-3</sup>	
mitochondrial concentration	$C_{mtE}$	$C_{mtE} = mtE \cdot V^{-1}$	mtEU · m <sup>-3</sup>	3
specific mitochondrial density	$D_{mtE}$	$D_{mtE} = mtE \cdot m_X^{-1}$	mtEU · kg <sup>-1</sup>	4
mitochondrial content, $mtE$ per object $X$	$mtE_X$	$mtE_X = mtE \cdot N_X^{-1}$	mtEU · x <sup>-1</sup>	5
<b>O<sub>2</sub> flow and flux</b>				
flow, system	$I_{O_2}$	internal flow	mol · s <sup>-1</sup>	6
volume-specific flux	$J_{V,O_2}$	$J_{V,O_2} = I_{O_2} \cdot V^{-1}$	mol · s <sup>-1</sup> · m <sup>-3</sup>	7
flow per object $X$	$I_{O_2/X}$	$I_{O_2/X} = J_{V,O_2} \cdot C_{NX}^{-1}$	mol · s <sup>-1</sup> · x <sup>-1</sup>	8
mass-specific flux	$J_{O_2/mX}$	$J_{O_2/mX} = J_{V,O_2} \cdot C_{mX}^{-1}$	mol · s <sup>-1</sup> · kg <sup>-1</sup>	9
mitochondria-specific flux	$J_{O_2/mtE}$	$J_{O_2/mtE} = J_{V,O_2} \cdot C_{mtE}^{-1}$	mol · s <sup>-1</sup> · mtEU <sup>-1</sup>	10

978 1 The *SI* prefix k is used for the *SI* base unit of mass (kg = 1,000 g). In praxis, various *SI* prefixes are  
 979 used for convenience, to make numbers easily readable, *e.g.*, 1 mg tissue, cell or mitochondrial mass  
 980 instead of 0.000001 kg.

- 981 2 In case sample  $X = \text{cells}$ , the object number concentration is  $C_{N_{\text{cell}}} = N_{\text{cell}} \cdot V^{-1}$ , and volume may be  
982 expressed in  $[\text{dm}^3 \equiv \text{L}]$  or  $[\text{cm}^3 = \text{mL}]$ . See **Table 5** for different object types.  
983 3 mt-concentration is an experimental variable, dependent on sample concentration: (1)  $C_{mtE} = mtE \cdot V^{-1}$ ;  
984 (2)  $C_{mtE} = mtE_X \cdot C_{NX}$ ; (3)  $C_{mtE} = C_{mX} \cdot D_{mtE}$ .  
985 4 If the amount of mitochondria,  $mtE$ , is expressed as mitochondrial mass, then  $D_{mtE}$  is the mass  
986 fraction of mitochondria in the sample. If  $mtE$  is expressed as mitochondrial volume,  $V_{mt}$ , and the  
987 mass of sample,  $m_X$ , is replaced by volume of sample,  $V_X$ , then  $D_{mtE}$  is the volume fraction of  
988 mitochondria in the sample.  
989 5  $mtE_X = mtE \cdot N_X^{-1} = C_{mtE} \cdot C_{NX}^{-1}$ .  
990 6  $O_2$  can be replaced by other chemicals B to study different reactions, e.g., ATP,  $H_2O_2$ , or  
991 compartmental translocations, e.g.,  $Ca^{2+}$ .  
992 7  $I_{O_2}$  and  $V$  are defined per instrument chamber as a system of constant volume (and constant  
993 temperature), which may be closed or open.  $I_{O_2}$  is abbreviated for  $I_{rO_2}$ , i.e., the metabolic or internal  
994  $O_2$  flow of the chemical reaction  $r$  in which  $O_2$  is consumed, hence the negative stoichiometric  
995 number,  $\nu_{O_2} = -1$ .  $I_{rO_2} = d_r n_{O_2} / dt \cdot \nu_{O_2}^{-1}$ . If  $r$  includes all chemical reactions in which  $O_2$  participates, then  
996  $d_r n_{O_2} = dn_{O_2} - d_e n_{O_2}$ , where  $dn_{O_2}$  is the change in the amount of  $O_2$  in the instrument chamber and  $d_e n_{O_2}$   
997 is the amount of  $O_2$  added externally to the system. At steady state, by definition  $dn_{O_2} = 0$ , hence  $d_r n_{O_2}$   
998  $= -d_e n_{O_2}$ .  
999 8  $J_{V,O_2}$  is an experimental variable, expressed per volume of the instrument chamber.  
1000 9  $I_{O_2X}$  is a physiological variable, depending on the size of entity  $X$ .  
1001 10 There are many ways to normalize for a mitochondrial marker, that are used in different experimental  
1002 approaches: (1)  $J_{O_2/mtE} = J_{V,O_2} \cdot C_{mtE}^{-1}$ ; (2)  $J_{O_2/mtE} = J_{V,O_2} \cdot C_{mX}^{-1} \cdot D_{mtE}^{-1} = J_{O_2/mX} \cdot D_{mtE}^{-1}$ ; (3)  $J_{O_2/mtE} =$   
1003  $J_{V,O_2} \cdot C_{NX}^{-1} \cdot mtE_X^{-1} = I_{O_2X} \cdot mtE_X^{-1}$ ; (4)  $J_{O_2/mtE} = I_{O_2} \cdot mtE^{-1}$ . The mt-elemental unit [mtEU] varies between  
1004 different mt-markers.  
1005  
1006

**Table 5. Sample types, X, abbreviations, and quantification.**

Identity of sample	X	$N_X$	Mass <sup>a</sup>	Volume	mt-Marker
mitochondrial preparation	mt-prep	[x]	[kg]	[m <sup>3</sup> ]	[mtEU]
isolated mitochondria	imt		$m_{mt}$	$V_{mt}$	$mtE$
tissue homogenate	thom		$m_{thom}$		$mtE_{thom}$
permeabilized tissue	pti		$m_{pti}$		$mtE_{pti}$
permeabilized fibre	pfi		$m_{pfi}$		$mtE_{pfi}$
permeabilized cell	pce	$N_{pce}$	$M_{pce}$	$V_{pce}$	$mtE_{pce}$
cells <sup>b</sup>	cell	$N_{cell}$	$M_{cell}$	$V_{cell}$	$mtE_{cell}$
intact cell, viable cell	vce	$N_{vce}$	$M_{vce}$	$V_{vce}$	
dead cell	dce	$N_{dce}$	$M_{dce}$	$V_{dce}$	
organism	org	$N_{org}$	$M_{org}$	$V_{org}$	

<sup>a</sup> Instead of mass, the wet weight or dry weight is frequently stated,  $W_w$  or  $W_d$ .

$m_X$  is mass of the sample [kg],  $M_X$  is mass of the object [ $\text{kg} \cdot \text{x}^{-1}$ ].

<sup>b</sup> Total cell count,  $N_{cell} = N_{vce} + N_{dce}$

Cellular  $O_2$  flow can be compared between cells of identical size. To take into account changes and differences in cell size, normalization is required to obtain cell size-specific or mitochondrial marker-specific  $O_2$  flux (Renner *et al.* 2003).

The complexity changes when the sample is a whole organism studied as an experimental model. The scaling law in respiratory physiology reveals a strong interaction of  $O_2$  flow and individual body mass of an organism, since *basal* metabolic rate (flow) does not increase linearly with body mass, whereas *maximum* mass-specific  $O_2$  flux,  $\dot{V}_{O_2\text{max}}$  or  $\dot{V}_{O_2\text{peak}}$ , is approximately constant across a large range of individual body mass (Weibel and Hoppeler 2005), with individuals, breeds, and species deviating substantially from this relationship.  $\dot{V}_{O_2\text{peak}}$  of human endurance athletes is 60 to 80 mL  $O_2 \cdot \text{min}^{-1} \cdot \text{kg}^{-1}$  body mass, converted to  $J_{O_2\text{peak}/M}$  of 45 to 60 nmol  $\cdot \text{s}^{-1} \cdot \text{g}^{-1}$  (Gnaiger 2014; **Table 6**).

### 3.4. Normalization for mitochondrial content

1025 Tissues can contain multiple cell populations that may have distinct mitochondrial  
 1026 subtypes. Mitochondria undergo dynamic fission and fusion cycles, and can exist in multiple  
 1027 stages and sizes that may be altered by a range of factors. The isolation of mitochondria (often  
 1028 achieved through differential centrifugation) can therefore yield a subsample of the  
 1029 mitochondrial types present in a tissue, depending on the isolation protocols utilized (*e.g.*,  
 1030 centrifugation speed). This possible bias should be taken into account when planning  
 1031 experiments using isolated mitochondria. Different sizes of mitochondria are enriched at  
 1032 specific centrifugation speeds, which can be used strategically for isolation of mitochondrial  
 1033 subpopulations.

1034 Part of the mitochondrial content of a tissue is lost during preparation of isolated  
 1035 mitochondria. The fraction of mitochondria in the isolate is expressed as mitochondrial  
 1036 recovery. At a high mitochondrial recovery the sample of isolated mitochondria is more  
 1037 representative of the total mitochondrial population than in preparations characterized by low  
 1038 recovery. Determination of the mitochondrial recovery and yield is based on measurement of  
 1039 the concentration of a mitochondrial marker in the tissue homogenate,  $C_{mtE,thom}$ , which  
 1040 simultaneously provides information on the specific mitochondrial density in the sample.  
 1041

<b>Flow, Performance</b>	=	<b>Element function</b>	x	<b>Element density</b>	x	<b>Size of object</b>
$\frac{\text{mol}\cdot\text{s}^{-1}}{x}$	=	$\frac{\text{mol}\cdot\text{s}^{-1}}{x_{mtE}}$	·	$\frac{x_{mtE}}{\text{kg}}$	·	$\frac{\text{kg}}{x}$

<b>A</b>	<b>Flow</b>	=	<b>mt-specific flux</b>	x	<b>mt-structure, functional elements</b>
	$I_{O_2/X}$	=	$J_{O_2/mtE}$	·	$mtE_X$
					$\frac{mtE_X}{M_X} \cdot M_X$

$I_{O_2/X}$	=	$J_{O_2/mtE}$	·	$D_{mtE}$	·	$M_X$
-------------	---	---------------	---	-----------	---	-------

$\frac{I_{O_2/X}}{M_X}$	=	$\frac{I_{O_2/X}}{mtE_X}$	·	$\frac{mtE_X}{M_X}$
-------------------------	---	---------------------------	---	---------------------

<b>B</b>	$I_{O_2/X}$	=	$J_{O_2/MX}$	·	$M_X$
	<b>Flow</b>	=	<b>Object mass- specific flux</b>	x	<b>Mass of object</b>

1042 **Fig. 7. Structure-function analysis of performance of an organism, organ or tissue, or a**  
 1043 **cell (sample entity, X). O<sub>2</sub> flow,  $I_{O_2/X}$ , is the product of performance per functional element**  
 1044 **(element function, mitochondria-specific flux), element density (mitochondrial density,**  
 1045  **$D_{mtE}$ ), and size of entity X (mass,  $M_X$ ). (A) Structured analysis: performance is the product of**  
 1046 **mitochondrial function (mt-specific flux) and structure (functional elements;  $D_{mtE}$  times mass**  
 1047 **of X). (B) Unstructured analysis: performance is the product of entity mass-specific flux,  $J_{O_2/MX}$**   
 1048  **$= I_{O_2/X}/M_X = I_{O_2}/m_X$  [mol·s<sup>-1</sup>·kg<sup>-1</sup>] and size of entity, expressed as mass of X;  $M_X = m_X \cdot N_X^{-1}$**   
 1049 **[kg·x<sup>-1</sup>]. See Table 4 for further explanation of quantities and units. Modified from Gnaiger**  
 1050 **(2014).**  
 1051

1052  
 1053 Normalization is a problematic subject; it is essential to consider the question of the study.  
 1054 If the study aims at comparing tissue performance—such as the effects of a treatment on a  
 1055 specific tissue, then normalization can be successful, using tissue mass or protein content, for  
 1056 example. However, if the aim is to find differences on mitochondrial function independent of  
 1057 mitochondrial density (Table 4), then normalization to a mitochondrial marker is imperative

1058 (Fig. 7). One cannot assume that quantitative changes in various markers—such as  
 1059 mitochondrial proteins—necessarily occur in parallel with one another. It should be established  
 1060 that the marker chosen is not selectively altered by the performed treatment. In conclusion, the  
 1061 normalization must reflect the question under investigation to reach a satisfying answer. On the  
 1062 other hand, the goal of comparing results across projects and institutions requires  
 1063 standardization on normalization for entry into a databank.

1064 **Mitochondrial concentration,  $C_{mtE}$ , and mitochondrial markers:** Mitochondrial  
 1065 organelles comprise a dynamic cellular reticulum in various states of fusion and fission. Hence,  
 1066 the definition of an "amount" of mitochondria is often misconceived: mitochondria cannot be  
 1067 counted reliably as a number of occurring elements. Therefore, quantification of the "amount"  
 1068 of mitochondria depends on the measurement of chosen mitochondrial markers. 'Mitochondria  
 1069 are the structural and functional elemental units of cell respiration' (Gnaiger 2014). The  
 1070 quantity of a mitochondrial marker can reflect the amount of *mitochondrial elements, mtE*,  
 1071 expressed in various mitochondrial elemental units [mtEU] specific for each measured mt-  
 1072 marker (Table 4). However, since mitochondrial quality may change in response to stimuli—  
 1073 particularly in mitochondrial dysfunction and after exercise training (Pesta *et al.* 2011; Campos  
 1074 *et al.* 2017)—some markers can vary while others are unchanged: (1) Mitochondrial volume  
 1075 and membrane area are structural markers, whereas mitochondrial protein mass is frequently  
 1076 used as a marker for isolated mitochondria. (2) Molecular and enzymatic mitochondrial markers  
 1077 (amounts or activities) can be selected as matrix markers, *e.g.*, citrate synthase activity, mtDNA;  
 1078 mtIM-markers, *e.g.*, cytochrome *c* oxidase activity, *aa<sub>3</sub>* content, cardiolipin, or mtOM-markers,  
 1079 *e.g.*, TOM20. (3) Extending the measurement of mitochondrial marker enzyme activity to  
 1080 mitochondrial pathway capacity, ET- or OXPHOS-capacity can be considered as an integrative  
 1081 functional mitochondrial marker.

1082 Depending on the type of mitochondrial marker, the mitochondrial elements, *mtE*, are  
 1083 expressed in marker-specific units. Mitochondrial concentration in the measurement chamber  
 1084 and the tissue of origin are quantified as (1) a quantity for normalization in functional analyses,  
 1085  $C_{mtE}$ , and (2) a physiological output that is the result of mitochondrial biogenesis and  
 1086 degradation,  $D_{mtE}$ , respectively (Table 4). It is recommended, therefore, to distinguish  
 1087 *experimental mitochondrial concentration*,  $C_{mtE} = mtE/V$  and *physiological mitochondrial*  
 1088 *density*,  $D_{mtE} = mtE/m_X$ . Then mitochondrial density is the amount of mitochondrial elements  
 1089 per mass of tissue, which is a biological variable (Fig. 7). The experimental variable is  
 1090 mitochondrial density multiplied by sample mass concentration in the measuring chamber,  $C_{mtE}$   
 1091  $= D_{mtE} \cdot C_{m_X}$ , or mitochondrial content multiplied by sample number concentration,  $C_{mtE} =$   
 1092  $mtE_X \cdot C_{N_X}$  (Table 4).

1093 **Mitochondria-specific flux,  $J_{O_2/mtE}$ :** Volume-specific metabolic  $O_2$  flux depends on: (1)  
 1094 the sample concentration in the volume of the instrument chamber,  $C_{m_X}$ , or  $C_{N_X}$ ; (2) the  
 1095 mitochondrial density in the sample,  $D_{mtE} = mtE/m_X$  or  $mtE_X = mtE/N_X$ ; and (3) the specific  
 1096 mitochondrial activity or performance per elemental mitochondrial unit,  $J_{O_2/mtE} = J_{V,O_2}/C_{mtE}$   
 1097  $[mol \cdot s^{-1} \cdot mtEU^{-1}]$  (Table 4). Obviously, the numerical results for  $J_{O_2/mtE}$  vary with the type of  
 1098 mitochondrial marker chosen for measurement of *mtE* and  $C_{mtE} = mtE/V$   $[mtEU \cdot m^{-3}]$ .

### 1099 3.5. Evaluation of mitochondrial markers

1100 Different methods are implicated in the quantification of mitochondrial markers and have  
 1101 different strengths. Some problems are common for all mitochondrial markers, *mtE*: (1)  
 1102 Accuracy of measurement is crucial, since even a highly accurate and reproducible  
 1103 measurement of  $O_2$  flux results in an inaccurate and noisy expression if normalized by a biased  
 1104 and noisy measurement of a mitochondrial marker. This problem is acute in mitochondrial  
 1105 respiration because the denominators used (the mitochondrial markers) are often small moieties  
 1106 of which accurate and precise determination is difficult. This problem can be avoided when  $O_2$   
 1107  
 1108



1109 fluxes measured in substrate-uncoupler-inhibitor titration protocols are normalized for flux in  
1110 a defined respiratory reference state, which is used as an *internal* marker and yields flux control  
1111 ratios, *FCRs*. *FCRs* are independent of *externally* measured markers and, therefore, are  
1112 statistically robust, considering the limitations of ratios in general (Jasienski and Bazzaz 1999).  
1113 *FCRs* indicate qualitative changes of mitochondrial respiratory control, with highest  
1114 quantitative resolution, separating the effect of mitochondrial density or concentration on  $J_{O_2/mX}$   
1115 and  $I_{O_2/X}$  from that of function per elemental mitochondrial marker,  $J_{O_2/mtE}$  (Pesta *et al.* 2011;  
1116 Gnaiger 2014). (2) If mitochondrial quality does not change and only the amount of  
1117 mitochondria varies as a determinant of mass-specific flux, any marker is equally qualified in  
1118 principle; then in practice selection of the optimum marker depends only on the accuracy and  
1119 precision of measurement of the mitochondrial marker. (3) If mitochondrial flux control ratios  
1120 change, then there may not be any best mitochondrial marker. In general, measurement of  
1121 multiple mitochondrial markers enables a comparison and evaluation of normalization for a  
1122 variety of mitochondrial markers. Particularly during postnatal development, the activity of  
1123 marker enzymes—such as cytochrome *c* oxidase and citrate synthase—follows different time  
1124 courses (Drahota *et al.* 2004). Evaluation of mitochondrial markers in healthy controls is  
1125 insufficient for providing guidelines for application in the diagnosis of pathological states and  
1126 specific treatments.

1127 In line with the concept of the respiratory control ratio (Chance and Williams 1955a), the  
1128 most readily used normalization is that of flux control ratios and flux control factors (Gnaiger  
1129 2014). Selection of the state of maximum flux in a protocol as the reference state has the  
1130 advantages of: (1) internal normalization; (2) statistical linearization of the response in the range  
1131 of 0 to 1; and (3) consideration of maximum flux for integrating a large number of elemental  
1132 steps in the OXPHOS- or ET-pathways. This reduces the risk of selecting a functional marker  
1133 that is specifically altered by the treatment or pathology, yet increases the chance that the highly  
1134 integrative pathway is disproportionately affected, *e.g.*, the OXPHOS- rather than ET-pathway  
1135 in case of an enzymatic defect in the phosphorylation-pathway. In this case, additional  
1136 information can be obtained by reporting flux control ratios based on a reference state which  
1137 indicates stable tissue-mass specific flux. Stereological determination of mitochondrial content  
1138 via two-dimensional transmission electron microscopy can have limitations due to the dynamics  
1139 of mitochondrial size (Meinild Lundby *et al.* 2017). Accurate determination of three-  
1140 dimensional volume by two-dimensional microscopy can be both time consuming and  
1141 statistically challenging (Larsen *et al.* 2012).

1142 The validity of using mitochondrial marker enzymes (citrate synthase activity, Complex  
1143 I–IV amount or activity) for normalization of flux is limited in part by the same factors that  
1144 apply to flux control ratios. Strong correlations between various mitochondrial markers and  
1145 citrate synthase activity (Reichmann *et al.* 1985; Boushel *et al.* 2007; Mogensen *et al.* 2007)  
1146 are expected in a specific tissue of healthy subjects and in disease states not specifically  
1147 targeting citrate synthase. Citrate synthase activity is acutely modifiable by exercise  
1148 (Tonkonogi *et al.* 1997; Leek *et al.* 2001). Evaluation of mitochondrial markers related to a  
1149 selected age and sex cohort cannot be extrapolated to provide recommendations for  
1150 normalization in respirometric diagnosis of disease, in different states of development and  
1151 ageing, different cell types, tissues, and species. mtDNA normalized to nDNA via qPCR is  
1152 correlated to functional mitochondrial markers including OXPHOS- and ET-capacity in some  
1153 cases (Puntschart *et al.* 1995; Wang *et al.* 1999; Menshikova *et al.* 2006; Boushel *et al.* 2007),  
1154 but lack of such correlations have been reported (Menshikova *et al.* 2005; Schultz and Wiesner  
1155 2000; Pesta *et al.* 2011). Several studies indicate a strong correlation between cardiolipin  
1156 content and increase in mitochondrial function with exercise (Menshikova *et al.* 2005;  
1157 Menshikova *et al.* 2007; Larsen *et al.* 2012; Faber *et al.* 2014), but it has not been evaluated as  
1158 a general mitochondrial biomarker in disease.  
1159



## 1160 3.6. Conversion: units

1161  
1162 Many different units have been used to report the O<sub>2</sub> consumption rate, OCR (**Table 6**).  
1163 *SI* base units provide the common reference to introduce the theoretical principles (**Fig. 6**), and  
1164 are used with appropriately chosen *SI* prefixes to express numerical data in the most practical  
1165 format, with an effort towards unification within specific areas of application (**Table 7**).  
1166 Reporting data in *SI* units—including the mole [mol], coulomb [C], joule [J], and second [s]—  
1167 should be encouraged, particularly by journals which propose the use of *SI* units.

1168 Although volume is expressed as m<sup>3</sup> using the *SI* base unit, the litre [dm<sup>3</sup>] is a  
1169 conventional unit of volume for concentration and is used for most solution chemical kinetics.  
1170 If one multiplies  $I_{O_2/cell}$  by  $C_{Ncell}$ , then the result will not only be the amount of O<sub>2</sub> [mol]  
1171 consumed per time [s<sup>-1</sup>] in one litre [L<sup>-1</sup>], but also the change in O<sub>2</sub> concentration per second  
1172 (for any volume of an ideally closed system). This is ideal for kinetic modeling as it blends with  
1173 chemical rate equations where concentrations are typically expressed in mol·L<sup>-1</sup> (Wagner *et al.*  
1174 2011). In studies of multinuclear cells—such as differentiated skeletal muscle cells—it is easy  
1175 to determine the number of nuclei but not the total number of cells. A generalized concept,  
1176 therefore, is obtained by substituting cells by nuclei as the sample entity. This does not hold,  
1177 however, for enucleated platelets.

1178  
1179 **Table 6. Conversion of various units used in respirometry and**  
1180 **ergometry.**  $e^-$  is the number of electrons or reducing equivalents.  $z_B$  is the  
1181 charge number of entity B.  
1182

1 Unit	x	Multiplication factor	<i>SI</i> -unit	Note
ng.atom O·s <sup>-1</sup>	(2 e <sup>-</sup> )	0.5	nmol O <sub>2</sub> ·s <sup>-1</sup>	
ng.atom O·min <sup>-1</sup>	(2 e <sup>-</sup> )	8.33	pmol O <sub>2</sub> ·s <sup>-1</sup>	
natom O·min <sup>-1</sup>	(2 e <sup>-</sup> )	8.33	pmol O <sub>2</sub> ·s <sup>-1</sup>	
nmol O <sub>2</sub> ·min <sup>-1</sup>	(4 e <sup>-</sup> )	16.67	pmol O <sub>2</sub> ·s <sup>-1</sup>	
nmol O <sub>2</sub> ·h <sup>-1</sup>	(4 e <sup>-</sup> )	0.2778	pmol O <sub>2</sub> ·s <sup>-1</sup>	
mL O <sub>2</sub> ·min <sup>-1</sup> at STPD <sup>a</sup>		0.744	μmol O <sub>2</sub> ·s <sup>-1</sup>	1
W = J/s at -470 kJ/mol O <sub>2</sub>		-2.128	μmol O <sub>2</sub> ·s <sup>-1</sup>	
mA = mC·s <sup>-1</sup>	(z <sub>H+</sub> = 1)	10.36	nmol H <sup>+</sup> ·s <sup>-1</sup>	2
mA = mC·s <sup>-1</sup>	(z <sub>O<sub>2</sub></sub> = 4)	2.59	nmol O <sub>2</sub> ·s <sup>-1</sup>	2
nmol H <sup>+</sup> ·s <sup>-1</sup>	(z <sub>H+</sub> = 1)	0.09649	mA	3
nmol O <sub>2</sub> ·s <sup>-1</sup>	(z <sub>O<sub>2</sub></sub> = 4)	0.38594	mA	3

1183 1 At standard temperature and pressure dry (STPD: 0 °C = 273.15 K and 1 atm =  
1184 101.325 kPa = 760 mmHg), the molar volume of an ideal gas,  $V_m$ , and  $V_{m,O_2}$  is  
1185 22.414 and 22.392 L·mol<sup>-1</sup>, respectively. Rounded to three decimal places, both  
1186 values yield the conversion factor of 0.744. For comparison at NTPD (20 °C),  
1187  $V_{m,O_2}$  is 24.038 L·mol<sup>-1</sup>. Note that the *SI* standard pressure is 100 kPa.

1188 2 The multiplication factor is  $10^6/(z_B \cdot F)$ .

1189 3 The multiplication factor is  $z_B \cdot F/10^6$ .

1190  
1191 For studies of cells, we recommend that respiration be expressed, as far as possible, as:  
1192 (1) O<sub>2</sub> flux normalized for a mitochondrial marker, for separation of the effects of mitochondrial  
1193 quality and content on cell respiration (this includes *FCRs* as a normalization for a functional  
1194 mitochondrial marker); (2) O<sub>2</sub> flux in units of cell volume or mass, for comparison of respiration  
1195 of cells with different cell size (Renner *et al.* 2003) and with studies on tissue preparations, and  
1196 (3) O<sub>2</sub> flow in units of attomole (10<sup>-18</sup> mol) of O<sub>2</sub> consumed in a second by each cell

1197 [amol·s<sup>-1</sup>·cell<sup>-1</sup>], numerically equivalent to [pmol·s<sup>-1</sup>·10<sup>-6</sup> cells]. This convention allows  
 1198 information to be easily used when designing experiments in which O<sub>2</sub> flow must be considered.  
 1199 For example, to estimate the volume-specific O<sub>2</sub> flux in an instrument chamber that would be  
 1200 expected at a particular cell number concentration, one simply needs to multiply the flow per  
 1201 cell by the number of cells per volume of interest. This provides the amount of O<sub>2</sub> [mol]  
 1202 consumed per time [s<sup>-1</sup>] per unit volume [L<sup>-1</sup>]. At an O<sub>2</sub> flow of 100 amol·s<sup>-1</sup>·cell<sup>-1</sup> and a cell  
 1203 density of 10<sup>9</sup> cells·L<sup>-1</sup> (10<sup>6</sup> cells·mL<sup>-1</sup>), the volume-specific O<sub>2</sub> flux is 100 nmol·s<sup>-1</sup>·L<sup>-1</sup> (100  
 1204 pmol·s<sup>-1</sup>·mL<sup>-1</sup>).

1205 ET-capacity in human cell types including HEK 293, primary HUVEC and fibroblasts  
 1206 ranges from 50 to 180 amol·s<sup>-1</sup>·cell<sup>-1</sup>, measured in intact cells in the noncoupled state (see  
 1207 Gnaiger 2014). At 100 amol·s<sup>-1</sup>·cell<sup>-1</sup> corrected for *Rox*, the current across the mt-membranes,  
 1208 *I<sub>H+e</sub>*, approximates 193 pA·cell<sup>-1</sup> or 0.2 nA per cell. See Rich (2003) for an extension of  
 1209 quantitative bioenergetics from the molecular to the human scale, with a transmembrane proton  
 1210 flux equivalent to 520 A in an adult at a catabolic power of -110 W. Modelling approaches  
 1211 illustrate the link between protonmotive force and currents (Willis *et al.* 2016).  
 1212

1213 **Table 7. Conversion of units with preservation of numerical values.**

Name	Frequently used unit	Equivalent unit	Note
volume-specific flux, $J_{V,O_2}$	pmol·s <sup>-1</sup> ·mL <sup>-1</sup> nmol·s <sup>-1</sup> ·L <sup>-1</sup>	nmol·s <sup>-1</sup> ·L <sup>-1</sup> mol·s <sup>-1</sup> ·m <sup>-3</sup>	1
cell-specific flow, $I_{O_2/cell}$	pmol·s <sup>-1</sup> ·10 <sup>-6</sup> cells pmol·s <sup>-1</sup> ·10 <sup>-9</sup> cells	amol·s <sup>-1</sup> ·cell <sup>-1</sup> zmol·s <sup>-1</sup> ·cell <sup>-1</sup>	2 3
cell number concentration, $C_{Nce}$	10 <sup>6</sup> cells·mL <sup>-1</sup>	10 <sup>9</sup> cells·L <sup>-1</sup>	
mitochondrial protein concentration, $C_{mtE}$	0.1 mg·mL <sup>-1</sup>	0.1 g·L <sup>-1</sup>	
mass-specific flux, $J_{O_2/m}$	pmol·s <sup>-1</sup> ·mg <sup>-1</sup>	nmol·s <sup>-1</sup> ·g <sup>-1</sup>	4
catabolic power, $P_k$	μW·10 <sup>-6</sup> cells	pW·cell <sup>-1</sup>	1
Volume	1,000 L L mL μL fL	m <sup>3</sup> (1,000 kg) dm <sup>3</sup> (kg) cm <sup>3</sup> (g) mm <sup>3</sup> (mg) μm <sup>3</sup> (pg)	5
amount of substance concentration	M = mol·L <sup>-1</sup>	mol·dm <sup>-3</sup>	

1214  
 1215 1 pmol: picomole = 10<sup>-12</sup> mol                      4 nmol: nanomole = 10<sup>-9</sup> mol  
 1216 2 amol: attomole = 10<sup>-18</sup> mol                      5 fL: femtolitre = 10<sup>-15</sup> L  
 1217 3 zmol: zeptomole = 10<sup>-21</sup> mol  
 1218

1219 We consider isolated mitochondria as powerhouses and proton pumps as molecular  
 1220 machines to relate experimental results to energy metabolism of the intact cell. The cellular  
 1221 P<sub>»</sub>/O<sub>2</sub> based on oxidation of glycogen is increased by the glycolytic (fermentative) substrate-  
 1222 level phosphorylation of 3 P<sub>»</sub>/Glyc or 0.5 mol P<sub>»</sub> for each mol O<sub>2</sub> consumed in the complete  
 1223 oxidation of a mol glycosyl unit (Glyc). Adding 0.5 to the mitochondrial P<sub>»</sub>/O<sub>2</sub> ratio of 5.4  
 1224 yields a bioenergetic cell physiological P<sub>»</sub>/O<sub>2</sub> ratio close to 6. Two NADH equivalents are  
 1225 formed during glycolysis and transported from the cytosol into the mitochondrial matrix, either  
 1226 by the malate-aspartate shuttle or by the glycerophosphate shuttle resulting in different  
 1227 theoretical yields of ATP generated by mitochondria, the energetic cost of which potentially  
 1228 must be taken into account. Considering also substrate-level phosphorylation in the TCA cycle,  
 1229 this high P<sub>»</sub>/O<sub>2</sub> ratio not only reflects proton translocation and OXPHOS studied in isolation,

1230 but integrates mitochondrial physiology with energy transformation in the living cell (Gnaiger  
1231 1993a).

1232

1233

#### 1234 4. Conclusions

1235

1236 MitoEAGLE can serve as a gateway to better diagnose mitochondrial respiratory defects  
1237 linked to genetic variation, age-related health risks, sex-specific mitochondrial performance,  
1238 lifestyle with its effects on degenerative diseases, and thermal and chemical environment. The  
1239 present recommendations on coupling control states and rates, linked to the concept of the  
1240 protonmotive force, are focused on studies with mitochondrial preparations. These will be  
1241 extended in a series of reports on pathway control of mitochondrial respiration, respiratory  
1242 states in intact cells, and harmonization of experimental procedures.

1243

1244

---

#### 1245 **Box 3: Mitochondrial and cell respiration**

1246

1247 Mitochondrial and cell respiration is the process of exergonic and exothermic energy  
1248 transformation in which scalar redox reactions are coupled to vectorial ion translocation across  
1249 a semipermeable membrane, which separates the small volume of a bacterial cell or  
1250 mitochondrion from the larger volume of its surroundings. The electrochemical exergy can be  
1251 partially conserved in the phosphorylation of ADP to ATP or in ion pumping, or dissipated in  
1252 an electrochemical short-circuit. Respiration is thus clearly distinguished from fermentation as  
1253 the counterpart of cellular core energy metabolism. Respiration is separated in mitochondrial  
1254 preparations from the partial contribution of fermentative pathways of the intact cell. Residual  
1255 O<sub>2</sub> consumption—as measured after inhibition of mitochondrial electron transfer—does not  
1256 belong to the class of catabolic reactions and is, therefore, subtracted from total O<sub>2</sub> consumption  
1257 to obtain baseline-corrected respiration.

1258 Mitochondrial dysfunction is associated with a wide variety of genetic and degenerative  
1259 diseases. Robust mitochondrial function is supported by physical exercise and caloric balance,  
1260 and is central for sustained metabolic health throughout life. Therefore, a consistent  
1261 presentation of mitochondrial physiology will improve our understanding of the etiology of  
1262 disease and the diagnostic repertoire of mitochondrial medicine, with a focus on protective  
1263 medicine, lifestyle and healthy aging.

1264

---

1265 The optimal choice for expressing mitochondrial and cell respiration (**Box 3**) as O<sub>2</sub> flow  
1266 per biological sample, and normalization for specific tissue-markers (volume, mass, protein)  
1267 and mitochondrial markers (volume, protein, content, mtDNA, activity of marker enzymes,  
1268 respiratory reference state) is guided by the scientific question under study. Interpretation of  
1269 the data depends critically on appropriate normalization.

1270 We recommend for studies with mitochondrial preparations:

- 1271 1. Normalization of respiratory rates should be provided as far as possible: (1) biophysical  
1272 normalization: on a per cell basis as O<sub>2</sub> flow (may not be possible when dealing with  
1273 tissues); (2) cellular normalization: per g cell or tissue protein, or per cell or tissue mass  
1274 as mass-specific O<sub>2</sub> flux; and (3) mitochondrial normalization: per mitochondrial marker  
1275 as mt-specific flux. With information on cell size and the use of multiple normalizations,  
1276 maximum potential information is available (Renner *et al.* 2003; Wagner *et al.* 2011;  
1277 Gnaiger 2014). Reporting flow in a respiratory chamber [nmol·s<sup>-1</sup>] is discouraged, since  
1278 it restricts the analysis to intra-experimental comparison of relative (qualitative)  
1279 differences.
- 1280

- 1281 2. Catabolic mitochondrial respiration is distinguished from residual oxygen consumption.  
 1282 Fluxes in mitochondrial coupling states should be, as far as possible, corrected for residual  
 1283 oxygen consumption.
- 1284 3. In studies of isolated mitochondria, the mitochondrial recovery and yield should be  
 1285 reported. Experimental criteria for evaluation of purity versus integrity should be  
 1286 considered. Mitochondrial markers—such as citrate synthase activity as an enzymatic  
 1287 matrix marker—provide a link to the tissue of origin on the basis of calculating the  
 1288 mitochondrial recovery, *i.e.*, the fraction of mitochondrial marker obtained from a unit  
 1289 mass of tissue. Total mitochondrial protein is frequently applied as a mitochondrial  
 1290 marker, which is restricted to isolated mitochondria.
- 1291 4. In studies of permeabilized cells, the viability of the cell culture or cell suspension of  
 1292 origin should be reported. Normalization should be evaluated for total cell count or viable  
 1293 cell count.
- 1294 5. Terms and symbols are summarized in **Table 8**. Their use will facilitate transdisciplinary  
 1295 communication and support further developments towards a consistent theory of  
 1296 bioenergetics and mitochondrial physiology.
- 1297 6. Technical terms related to and defined with normal words can be used as index terms in  
 1298 databases, support the creation of ontologies towards semantic information processing  
 1299 (MitoPedia), and help in communicating analytical findings as impactful data-driven  
 1300 stories. ‘*Making data available without making it understandable may be worse than not*  
 1301 *making it available at all*’ (National Academies of Sciences, Engineering, and Medicine  
 1302 2018). This is a call to carefully contribute to FAIR principles (Findable, Accessible,  
 1303 Interoperable, Reusable) for the sharing of scientific data.

1304  
 1305 **Table 8. Terms, symbols, and units.**  
 1306  
 1307

1308 Term	Symbol	Unit	Links and comments
1310 alternative quinol oxidase	AOX		Fig. 1
1311 amount of substance B	$n_B$	[mol]	
1312 cell number	$N_{\text{cell}}$	[x]	Tab. 5; $N_{\text{cell}} = N_{\text{vce}} + N_{\text{dce}}$
1313 cell viability index	$CVI$		$CVI = N_{\text{vce}}/N_{\text{cell}} = 1 - N_{\text{dce}}/N_{\text{cell}}$
1314 Complexes I to IV	CI to CIV		respiratory ET Complexes; Fig. 1
1315 concentration of substance B	$c_B = n_B \cdot V^{-1}$ ; [B]	[mol·m <sup>-3</sup> ]	Box 2
1316 dead cell number	$N_{\text{dce}}$	[x]	Tab. 5; non-viable cells, loss of plasma membrane barrier function
1317 electron transfer system	ETS		Fig. 1, Fig. 4
1318 flow, for substance B	$I_B$	[mol·s <sup>-1</sup> ]	system-related extensive quantity; Fig. 6
1319 flux, for substance B	$J_B$	<i>varies</i>	size-specific quantity; Fig. 6
1320 inorganic phosphate	$P_i$		Fig. 2
1321 intact cell number, viable cell number	$N_{\text{vce}}$	[x]	Tab. 5; viable cells, intact of plasma membrane barrier function
1322 LEAK	LEAK		Tab. 1, Fig. 4
1323 mass of sample $X$	$m_X$	[kg]	Tab. 4
1324 mass of entity $X$	$M_X$	[kg]	mass of object $X$ ; Tab. 4
1325 MITOCARTA			<a href="https://www.broadinstitute.org/scientific-community/science/programs/metabolic-disease-program/publications/mitocarta/mitocarta-in-0">https://www.broadinstitute.org/scientific-community/science/programs/metabolic-disease-program/publications/mitocarta/mitocarta-in-0</a>
1326 MitoPedia			<a href="http://www.bioblast.at/index.php/MitoPedia">http://www.bioblast.at/index.php/MitoPedia</a>
1327 mitochondria or mitochondrial	mt		Box 1
1328 mitochondrial DNA	mtDNA		Box 1
1329 mitochondrial concentration	$C_{\text{mtE}} = \text{mtE} \cdot V^{-1}$	[mtEU·m <sup>-3</sup> ]	Tab. 4
1330 mitochondrial content	$\text{mtE}_X = \text{mtE} \cdot N_X^{-1}$	[mtEU·x <sup>-1</sup> ]	Tab. 4

1338	mitochondrial elemental unit	mtEU	<i>varies</i>	Tab. 4, specific units for mt-marker
1339	mitochondrial inner membrane	mtIM		MIM is widely used; the first M is replaced by mt; Box 1
1340				
1341	mitochondrial outer membrane	mtOM		MOM is widely used; the first M is replaced by mt; Box 1
1342				
1343	mitochondrial recovery	$Y_{mtE}$		fraction of <i>mtE</i> recovered in sample from the tissue of origin
1344				
1345	mitochondrial yield	$Y_{mtE/m}$		$Y_{mtE/m} = Y_{mtE} \cdot D_{mtE}$
1346	negative	neg		Fig. 2
1347	number concentration of <i>X</i>	$C_{NX}$	$[x \cdot m^{-3}]$	Tab. 4
1348	number of entities <i>X</i>	$N_X$	$[x]$	Tab. 4, Fig. 7
1349	number of entity <i>B</i>	$N_B$	$[x]$	Tab. 4
1350	oxidative phosphorylation	OXPPOS		Tab. 1, Fig. 4
1351	oxygen concentration	$c_{O_2} = n_{O_2} \cdot V^{-1}$ ; $[O_2]$	$[mol \cdot m^{-3}]$	Section 3.2
1352	permeabilized cell number	$N_{pce}$	$[x]$	Tab. 5; experimental permeabilization of plasma membrane; $N_{pce} = N_{cell}$
1353				
1354	phosphorylation of ADP to ATP	P»		Section 2.2
1355	positive	pos		Fig. 2
1356	proton in the negative compartment	$H^{+neg}$		Fig. 2
1357	proton in the positive compartment	$H^{+pos}$		Fig. 2
1358	rate of electron transfer in ET state	<i>E</i>		ET-capacity; Tab. 1
1359	rate of LEAK respiration	<i>L</i>		Tab. 1
1360	rate of oxidative phosphorylation	<i>P</i>		OXPPOS capacity; Tab. 1
1361	rate of residual oxygen consumption	<i>Rox</i>		Tab. 1
1362	residual oxygen consumption	ROX		Tab. 1
1363	respiratory supercomplex	SC I <sub>n</sub> III <sub>n</sub> IV <sub>n</sub>		Box 1; supramolecular assemblies composed of variable copy numbers ( <i>n</i> ) of CI, CIII and CIV
1364				
1365				
1366	specific mitochondrial density	$D_{mtE} = mtE \cdot m_X^{-1}$	$[mtEU \cdot kg^{-1}]$	Tab. 4
1367	volume	<i>V</i>	$[m^{-3}]$	Tab. 7
1368	weight, dry weight	$W_d$	$[kg]$	used as mass of sample <i>X</i> ; Fig. 6
1369	weight, wet weight	$W_w$	$[kg]$	used as mass of sample <i>X</i> ; Fig. 6
1370				

1371

## 1372 Acknowledgements

1373 We thank M. Beno for management assistance. Supported by COST Action CA15203  
1374 MitoEAGLE and K-Regio project MitoFit (E.G.).

1375

1376 **Competing financial interests:** E.G. is founder and CEO of Oroboros Instruments, Innsbruck,  
1377 Austria.

1378

1379

## 1380 5. References

1381

1382 Altmann R (1894) Die Elementarorganismen und ihre Beziehungen zu den Zellen. Zweite vermehrte Auflage.

1383 Verlag Von Veit & Comp, Leipzig:160 pp.

1384 Beard DA (2005) A biophysical model of the mitochondrial respiratory system and oxidative phosphorylation.

1385 PLoS Comput Biol 1(4):e36.

1386 Benda C (1898) Weitere Mitteilungen über die Mitochondria. Verh Dtsch Physiol Ges:376-83.

1387 Birkedal R, Laasmaa M, Vendelin M (2014) The location of energetic compartments affects energetic

1388 communication in cardiomyocytes. Front Physiol 5:376.

1389 Breton S, Beaupré HD, Stewart DT, Hoeh WR, Blier PU (2007) The unusual system of doubly uniparental

1390 inheritance of mtDNA: isn't one enough? Trends Genet 23:465-74.

1391 Brown GC (1992) Control of respiration and ATP synthesis in mammalian mitochondria and cells. Biochem J

1392 284:1-13.

1393 Calvo SE, Klauser CR, Mootha VK (2016) MitoCarta2.0: an updated inventory of mammalian mitochondrial

1394 proteins. Nucleic Acids Research 44:D1251-7.

1395 Calvo SE, Julien O, Clauser KR, Shen H, Kamer KJ, Wells JA, Mootha VK (2017) Comparative analysis of

1396 mitochondrial N-termini from mouse, human, and yeast. Mol Cell Proteomics 16:512-23.



- 1397 Campos JC, Queliconi BB, Bozi LHM, Bechara LRG, Dourado PMM, Andres AM, Jannig PR, Gomes KMS,  
 1398 Zambelli VO, Rocha-Resende C, Guatimosim S, Brum PC, Mochly-Rosen D, Gottlieb RA, Kowaltowski AJ,  
 1399 Ferreira JCB (2017) Exercise reestablishes autophagic flux and mitochondrial quality control in heart failure.  
 1400 *Autophagy* 13:1304-317.
- 1401 Canton M, Luvisetto S, Schmehl I, Azzone GF (1995) The nature of mitochondrial respiration and  
 1402 discrimination between membrane and pump properties. *Biochem J* 310:477-81.
- 1403 Chance B, Williams GR (1955a) Respiratory enzymes in oxidative phosphorylation. I. Kinetics of oxygen  
 1404 utilization. *J Biol Chem* 217:383-93.
- 1405 Chance B, Williams GR (1955b) Respiratory enzymes in oxidative phosphorylation: III. The steady state. *J Biol*  
 1406 *Chem* 217:409-27.
- 1407 Chance B, Williams GR (1955c) Respiratory enzymes in oxidative phosphorylation. IV. The respiratory chain. *J*  
 1408 *Biol Chem* 217:429-38.
- 1409 Chance B, Williams GR (1956) The respiratory chain and oxidative phosphorylation. *Adv Enzymol Relat Subj*  
 1410 *Biochem* 17:65-134.
- 1411 Cobb LJ, Lee C, Xiao J, Yen K, Wong RG, Nakamura HK, Mehta HH, Gao Q, Ashur C, Huffman DM, Wan J,  
 1412 Muzumdar R, Barzilai N, Cohen P (2016) Naturally occurring mitochondrial-derived peptides are age-  
 1413 dependent regulators of apoptosis, insulin sensitivity, and inflammatory markers. *Aging (Albany NY)* 8:796-  
 1414 809.
- 1415 Cohen ER, Cvitas T, Frey JG, Holmström B, Kuchitsu K, Marquardt R, Mills I, Pavese F, Quack M, Stohner J,  
 1416 Strauss HL, Takami M, Thor HL (2008) Quantities, units and symbols in physical chemistry, IUPAC Green  
 1417 Book, 3rd Edition, 2nd Printing, IUPAC & RSC Publishing, Cambridge.
- 1418 Cooper H, Hedges LV, Valentine JC, eds (2009) *The handbook of research synthesis and meta-analysis*. Russell  
 1419 Sage Foundation.
- 1420 Coopersmith J (2010) *Energy, the subtle concept. The discovery of Feynman's blocks from Leibnitz to Einstein*.  
 1421 Oxford University Press:400 pp.
- 1422 Cummins J (1998) Mitochondrial DNA in mammalian reproduction. *Rev Reprod* 3:172-82.
- 1423 Dai Q, Shah AA, Garde RV, Yonish BA, Zhang L, Medvitz NA, Miller SE, Hansen EL, Dunn CN, Price TM  
 1424 (2013) A truncated progesterone receptor (PR-M) localizes to the mitochondrion and controls cellular  
 1425 respiration. *Mol Endocrinol* 27:741-53.
- 1426 Divakaruni AS, Brand MD (2011) The regulation and physiology of mitochondrial proton leak. *Physiology*  
 1427 (Bethesda) 26:192-205.
- 1428 Doerrier C, Garcia-Souza LF, Krumschnabel G, Wohlfarter Y, Mészáros AT, Gnaiger E (2018) High-Resolution  
 1429 FluoRespirometry and OXPHOS protocols for human cells, permeabilized fibres from small biopsies of  
 1430 muscle and isolated mitochondria. *Methods Mol. Biol.* (in press)
- 1431 Doskey CM, van 't Erve TJ, Wagner BA, Buettner GR (2015) Moles of a substance per cell is a highly  
 1432 informative dosing metric in cell culture. *PLOS ONE* 10:e0132572.
- 1433 Drahota Z, Milerová M, Stieglerová A, Houstek J, Ostádal B (2004) Developmental changes of cytochrome *c*  
 1434 oxidase and citrate synthase in rat heart homogenate. *Physiol Res* 53:119-22.
- 1435 Duarte FV, Palmeira CM, Rolo AP (2014) The role of microRNAs in mitochondria: small players acting wide.  
 1436 *Genes (Basel)* 5:865-86.
- 1437 Ernster L, Schatz G (1981) Mitochondria: a historical review. *J Cell Biol* 91:227s-55s.
- 1438 Estabrook RW (1967) Mitochondrial respiratory control and the polarographic measurement of ADP:O ratios.  
 1439 *Methods Enzymol* 10:41-7.
- 1440 Faber C, Zhu ZJ, Castellino S, Wagner DS, Brown RH, Peterson RA, Gates L, Barton J, Bickett M, Hagerty L,  
 1441 Kimbrough C, Sola M, Bailey D, Jordan H, Elangbam CS (2014) Cardiolipin profiles as a potential  
 1442 biomarker of mitochondrial health in diet-induced obese mice subjected to exercise, diet-restriction and  
 1443 ephedrine treatment. *J Appl Toxicol* 34:1122-9.
- 1444 Fell D (1997) *Understanding the control of metabolism*. Portland Press.
- 1445 Garlid KD, Beavis AD, Ratkje SK (1989) On the nature of ion leaks in energy-transducing membranes. *Biochim*  
 1446 *Biophys Acta* 976:109-20.
- 1447 Garlid KD, Semrad C, Zinchenko V. Does redox slip contribute significantly to mitochondrial respiration? In:  
 1448 Schuster S, Rigoulet M, Ouhabi R, Mazat J-P, eds (1993) *Modern trends in biothermokinetics*. Plenum Press,  
 1449 New York, London:287-93.
- 1450 Gerö D, Szabo C (2016) Glucocorticoids suppress mitochondrial oxidant production via upregulation of  
 1451 uncoupling protein 2 in hyperglycemic endothelial cells. *PLoS One* 11:e0154813.
- 1452 Gnaiger E. Efficiency and power strategies under hypoxia. Is low efficiency at high glycolytic ATP production a  
 1453 paradox? In: *Surviving Hypoxia: Mechanisms of Control and Adaptation*. Hochachka PW, Lutz PL, Sick T,  
 1454 Rosenthal M, Van den Thillart G, eds (1993a) CRC Press, Boca Raton, Ann Arbor, London, Tokyo:77-109.
- 1455 Gnaiger E (1993b) Nonequilibrium thermodynamics of energy transformations. *Pure Appl Chem* 65:1983-2002.
- 1456 Gnaiger E (2001) Bioenergetics at low oxygen: dependence of respiration and phosphorylation on oxygen and  
 1457 adenosine diphosphate supply. *Respir Physiol* 128:277-97.

- 1458 Gnaiger E (2009) Capacity of oxidative phosphorylation in human skeletal muscle. New perspectives of  
1459 mitochondrial physiology. *Int J Biochem Cell Biol* 41:1837-45.
- 1460 Gnaiger E (2014) Mitochondrial pathways and respiratory control. An introduction to OXPHOS analysis. 4th ed.  
1461 Mitochondr Physiol Network 19.12. Oroboros MiPNet Publications, Innsbruck:80 pp.
- 1462 Gnaiger E, Méndez G, Hand SC (2000) High phosphorylation efficiency and depression of uncoupled respiration  
1463 in mitochondria under hypoxia. *Proc Natl Acad Sci USA* 97:11080-5.
- 1464 Greggio C, Jha P, Kulkarni SS, Lagarrigue S, Broskey NT, Boutant M, Wang X, Conde Alonso S, Ofori E,  
1465 Auwerx J, Cantó C, Amati F (2017) Enhanced respiratory chain supercomplex formation in response to  
1466 exercise in human skeletal muscle. *Cell Metab* 25:301-11.
- 1467 Hinkle PC (2005) P/O ratios of mitochondrial oxidative phosphorylation. *Biochim Biophys Acta* 1706:1-11.
- 1468 Hofstadter DR (1979) Gödel, Escher, Bach: An eternal golden braid. A metaphorical fugue on minds and  
1469 machines in the spirit of Lewis Carroll. Harvester Press:499 pp.
- 1470 Illaste A, Laasmaa M, Peterson P, Vendelin M (2012) Analysis of molecular movement reveals latticelike  
1471 obstructions to diffusion in heart muscle cells. *Biophys J* 102:739-48.
- 1472 Jasienski M, Bazzaz FA (1999) The fallacy of ratios and the testability of models in biology. *Oikos* 84:321-26.
- 1473 Jepihhina N, Beraud N, Sepp M, Birkedal R, Vendelin M (2011) Permeabilized rat cardiomyocyte response  
1474 demonstrates intracellular origin of diffusion obstacles. *Biophys J* 101:2112-21.
- 1475 Klepinin A, Ounpuu L, Guzun R, Chekulayev V, Timohhina N, Tepp K, Shevchuk I, Schlattner U, Kaambre T  
1476 (2016) Simple oxygraphic analysis for the presence of adenylate kinase 1 and 2 in normal and tumor cells. *J*  
1477 *Bioenerg Biomembr* 48:531-48.
- 1478 Klingenberg M (2017) UCP1 - A sophisticated energy valve. *Biochimie* 134:19-27.
- 1479 Koit A, Shevchuk I, Ounpuu L, Klepinin A, Chekulayev V, Timohhina N, Tepp K, Puurand M, Truu L, Heck K,  
1480 Valvere V, Guzun R, Kaambre T (2017) Mitochondrial respiration in human colorectal and breast cancer  
1481 clinical material is regulated differently. *Oxid Med Cell Longev* 1372640.
- 1482 Komlódi T, Tretter L (2017) Methylene blue stimulates substrate-level phosphorylation catalysed by succinyl-  
1483 CoA ligase in the citric acid cycle. *Neuropharmacology* 123:287-98.
- 1484 Lane N (2005) Power, sex, suicide: mitochondria and the meaning of life. Oxford University Press:354 pp.
- 1485 Larsen S, Nielsen J, Neigaard Nielsen C, Nielsen LB, Wibrand F, Stride N, Schroder HD, Boushel RC, Helge  
1486 JW, Dela F, Hey-Mogensen M (2012) Biomarkers of mitochondrial content in skeletal muscle of healthy  
1487 young human subjects. *J Physiol* 590:3349-60.
- 1488 Lee C, Zeng J, Drew BG, Sallam T, Martin-Montalvo A, Wan J, Kim SJ, Mehta H, Hevener AL, de Cabo R,  
1489 Cohen P (2015) The mitochondrial-derived peptide MOTS-c promotes metabolic homeostasis and reduces  
1490 obesity and insulin resistance. *Cell Metab* 21:443-54.
- 1491 Lee SR, Kim HK, Song IS, Youm J, Dizon LA, Jeong SH, Ko TH, Heo HJ, Ko KS, Rhee BD, Kim N, Han J  
1492 (2013) Glucocorticoids and their receptors: insights into specific roles in mitochondria. *Prog Biophys Mol*  
1493 *Biol* 112:44-54.
- 1494 Leek BT, Mudaliar SR, Henry R, Mathieu-Costello O, Richardson RS (2001) Effect of acute exercise on citrate  
1495 synthase activity in untrained and trained human skeletal muscle. *Am J Physiol Regul Integr Comp Physiol*  
1496 280:R441-7.
- 1497 Lemieux H, Blier PU, Gnaiger E (2017) Remodeling pathway control of mitochondrial respiratory capacity by  
1498 temperature in mouse heart: electron flow through the Q-junction in permeabilized fibers. *Sci Rep* 7:2840.
- 1499 Lenaz G, Tioli G, Falasca AI, Genova ML (2017) Respiratory supercomplexes in mitochondria. In: Mechanisms  
1500 of primary energy trasduction in biology. M Wikstrom (ed) Royal Society of Chemistry Publishing, London,  
1501 UK:296-337.
- 1502 Margulis L (1970) Origin of eukaryotic cells. New Haven: Yale University Press.
- 1503 Meinild Lundby AK, Jacobs RA, Gehrig S, de Leur J, Hauser M, Bonne TC, Flück D, Dandanell S, Kirk N,  
1504 Kaech A, Ziegler U, Larsen S, Lundby C (2018) Exercise training increases skeletal muscle mitochondrial  
1505 volume density by enlargement of existing mitochondria and not de novo biogenesis. *Acta Physiol* 222,  
1506 e12905.
- 1507 Menshikova EV, Ritov VB, Fairfull L, Ferrell RE, Kelley DE, Goodpaster BH (2006) Effects of exercise on  
1508 mitochondrial content and function in aging human skeletal muscle. *J Gerontol A Biol Sci Med Sci* 61:534-  
1509 40.
- 1510 Menshikova EV, Ritov VB, Ferrell RE, Azuma K, Goodpaster BH, Kelley DE (2007) Characteristics of skeletal  
1511 muscle mitochondrial biogenesis induced by moderate-intensity exercise and weight loss in obesity. *J Appl*  
1512 *Physiol* (1985) 103:21-7.
- 1513 Menshikova EV, Ritov VB, Toledo FG, Ferrell RE, Goodpaster BH, Kelley DE (2005) Effects of weight loss  
1514 and physical activity on skeletal muscle mitochondrial function in obesity. *Am J Physiol Endocrinol Metab*  
1515 288:E818-25.
- 1516 Miller GA (1991) The science of words. Scientific American Library New York:276 pp.
- 1517 Mitchell P (1961) Coupling of phosphorylation to electron and hydrogen transfer by a chemi-osmotic type of  
1518 mechanism. *Nature* 191:144-8.

- 1519 Mitchell P (2011) Chemiosmotic coupling in oxidative and photosynthetic phosphorylation. *Biochim Biophys*  
 1520 *Acta Bioenergetics* 1807:1507-38.
- 1521 Mogensen M, Sahlin K, Fernström M, Glintborg D, Vind BF, Beck-Nielsen H, Højlund K (2007) Mitochondrial  
 1522 respiration is decreased in skeletal muscle of patients with type 2 diabetes. *Diabetes* 56:1592-9.
- 1523 Mohr PJ, Phillips WD (2015) Dimensionless units in the SI. *Metrologia* 52:40-7.
- 1524 Moreno M, Giacco A, Di Munno C, Goglia F (2017) Direct and rapid effects of 3,5-diiodo-L-thyronine (T2).  
 1525 *Mol Cell Endocrinol* 7207:30092-8.
- 1526 Morrow RM, Picard M, Derbeneva O, Leipzig J, McManus MJ, Gousspillou G, Barbat-Artigas S, Dos Santos C,  
 1527 Hepple RT, Murdock DG, Wallace DC (2017) Mitochondrial energy deficiency leads to hyperproliferation of  
 1528 skeletal muscle mitochondria and enhanced insulin sensitivity. *Proc Natl Acad Sci U S A* 114:2705-10.
- 1529 Murley A, Nunnari J (2016) The emerging network of mitochondria-organelle contacts. *Mol Cell* 61:648-53.
- 1530 National Academies of Sciences, Engineering, and Medicine (2018) International coordination for science data  
 1531 infrastructure: Proceedings of a workshop—in brief. Washington, DC: The National Academies Press. doi:  
 1532 <https://doi.org/10.17226/25015>.
- 1533 Paradies G, Paradies V, De Benedictis V, Ruggiero FM, Petrosillo G (2014) Functional role of cardiolipin in  
 1534 mitochondrial bioenergetics. *Biochim Biophys Acta* 1837:408-17.
- 1535 Pesta D, Gnaiger E (2012) High-Resolution Respirometry. OXPHOS protocols for human cells and  
 1536 permeabilized fibres from small biopsies of human muscle. *Methods Mol Biol* 810:25-58.
- 1537 Pesta D, Hoppel F, Macek C, Messner H, Faulhaber M, Kobel C, Parson W, Burtscher M, Schocke M, Gnaiger  
 1538 E (2011) Similar qualitative and quantitative changes of mitochondrial respiration following strength and  
 1539 endurance training in normoxia and hypoxia in sedentary humans. *Am J Physiol Regul Integr Comp Physiol*  
 1540 301:R1078–87.
- 1541 Price TM, Dai Q (2015) The role of a mitochondrial progesterone receptor (PR-M) in progesterone action.  
 1542 *Semin Reprod Med* 33:185-94.
- 1543 Puchowicz MA, Varnes ME, Cohen BH, Friedman NR, Kerr DS, Hoppel CL (2004) Oxidative phosphorylation  
 1544 analysis: assessing the integrated functional activity of human skeletal muscle mitochondria – case studies.  
 1545 *Mitochondrion* 4:377-85. Puntschart A, Claassen H, Jostarndt K, Hoppeler H, Billeter R (1995) mRNAs of  
 1546 enzymes involved in energy metabolism and mtDNA are increased in endurance-trained athletes. *Am J*  
 1547 *Physiol* 269:C619-25.
- 1548 Quiros PM, Mottis A, Auwerx J (2016) Mitonuclear communication in homeostasis and stress. *Nat Rev Mol*  
 1549 *Cell Biol* 17:213-26.
- 1550 Rackham O, Mercer TR, Filipovska A (2012) The human mitochondrial transcriptome and the RNA-binding  
 1551 proteins that regulate its expression. *WIREs RNA* 3:675–95.
- 1552 Reichmann H, Hoppeler H, Mathieu-Costello O, von Bergen F, Pette D (1985) Biochemical and ultrastructural  
 1553 changes of skeletal muscle mitochondria after chronic electrical stimulation in rabbits. *Pflugers Arch* 404:1-  
 1554 9.
- 1555 Renner K, Amberger A, Konwalinka G, Gnaiger E (2003) Changes of mitochondrial respiration, mitochondrial  
 1556 content and cell size after induction of apoptosis in leukemia cells. *Biochim Biophys Acta* 1642:115-23.
- 1557 Rich P (2003) Chemiosmotic coupling: The cost of living. *Nature* 421:583.
- 1558 Rostovtseva TK, Sheldon KL, Hassanzadeh E, Monge C, Saks V, Bezrukov SM, Sackett DL (2008) Tubulin  
 1559 binding blocks mitochondrial voltage-dependent anion channel and regulates respiration. *Proc Natl Acad Sci*  
 1560 *USA* 105:18746-51.
- 1561 Rustin P, Parfait B, Chretien D, Bourgeron T, Djouadi F, Bastin J, Rötig A, Munnich A (1996) Fluxes of  
 1562 nicotinamide adenine dinucleotides through mitochondrial membranes in human cultured cells. *J Biol Chem*  
 1563 271:14785-90.
- 1564 Saks VA, Veksler VI, Kuznetsov AV, Kay L, Sikk P, Tiivel T, Tranqui L, Olivares J, Winkler K, Wiedemann F,  
 1565 Kunz WS (1998) Permeabilised cell and skinned fiber techniques in studies of mitochondrial function in  
 1566 vivo. *Mol Cell Biochem* 184:81-100.
- 1567 Salabei JK, Gibb AA, Hill BG (2014) Comprehensive measurement of respiratory activity in permeabilized cells  
 1568 using extracellular flux analysis. *Nat Protoc* 9:421-38.
- 1569 Sazanov LA (2015) A giant molecular proton pump: structure and mechanism of respiratory complex I. *Nat Rev*  
 1570 *Mol Cell Biol* 16:375-88.
- 1571 Schneider TD (2006) Claude Shannon: biologist. The founder of information theory used biology to formulate  
 1572 the channel capacity. *IEEE Eng Med Biol Mag* 25:30-3.
- 1573 Schönfeld P, Dymkowska D, Wojtczak L (2009) Acyl-CoA-induced generation of reactive oxygen species in  
 1574 mitochondrial preparations is due to the presence of peroxisomes. *Free Radic Biol Med* 47:503-9.
- 1575 Schultz J, Wiesner RJ (2000) Proliferation of mitochondria in chronically stimulated rabbit skeletal muscle--  
 1576 transcription of mitochondrial genes and copy number of mitochondrial DNA. *J Bioenerg Biomembr* 32:627-  
 1577 34.
- 1578 Simson P, Jephthina N, Laasmaa M, Peterson P, Birkedal R, Vendelin M (2016) Restricted ADP movement in  
 1579 cardiomyocytes: Cytosolic diffusion obstacles are complemented with a small number of open mitochondrial  
 1580 voltage-dependent anion channels. *J Mol Cell Cardiol* 97:197-203.

- 1581 Stucki JW, Ineichen EA (1974) Energy dissipation by calcium recycling and the efficiency of calcium transport  
1582 in rat-liver mitochondria. *Eur J Biochem* 48:365-75.
- 1583 Tonkonogi M, Harris B, Sahlin K (1997) Increased activity of citrate synthase in human skeletal muscle after a  
1584 single bout of prolonged exercise. *Acta Physiol Scand* 161:435-6.
- 1585 Waczulikova I, Habodaszova D, Cagalinec M, Ferko M, Ulicna O, Mateasik A, Sikurova L, Ziegelhöffer A  
1586 (2007) Mitochondrial membrane fluidity, potential, and calcium transients in the myocardium from acute  
1587 diabetic rats. *Can J Physiol Pharmacol* 85:372-81.
- 1588 Wagner BA, Venkataraman S, Buettner GR (2011) The rate of oxygen utilization by cells. *Free Radic Biol Med*  
1589 51:700-712.
- 1590 Wang H, Hiatt WR, Barstow TJ, Brass EP (1999) Relationships between muscle mitochondrial DNA content,  
1591 mitochondrial enzyme activity and oxidative capacity in man: alterations with disease. *Eur J Appl Physiol*  
1592 *Occup Physiol* 80:22-7.
- 1593 Watt IN, Montgomery MG, Runswick MJ, Leslie AG, Walker JE (2010) Bioenergetic cost of making an  
1594 adenosine triphosphate molecule in animal mitochondria. *Proc Natl Acad Sci U S A* 107:16823-7.
- 1595 Weibel ER, Hoppeler H (2005) Exercise-induced maximal metabolic rate scales with muscle aerobic capacity. *J*  
1596 *Exp Biol* 208:1635-44.
- 1597 White DJ, Wolff JN, Pierson M, Gemmell NJ (2008) Revealing the hidden complexities of mtDNA inheritance.  
1598 *Mol Ecol* 17:4925-42.
- 1599 Wikström M, Hummer G (2012) Stoichiometry of proton translocation by respiratory complex I and its  
1600 mechanistic implications. *Proc Natl Acad Sci U S A* 109:4431-6.
- 1601 Willis WT, Jackman MR, Messer JI, Kuzmiak-Glancy S, Glancy B (2016) A simple hydraulic analog model of  
1602 oxidative phosphorylation. *Med Sci Sports Exerc* 48:990-1000.